US 20170373331A1

(19) United States

(12) Patent Application Publication (10) Pub. No.: US 2017/0373331 A1

AOKI (43) Pub. Date: Dec. 28, 2017

(54) **STATE DETECTION DEVICE AND METHOD FOR FUEL CELL**

(71) Applicant: **NISSAN MOTOR CO., LTD.**, Yokohama-shi, Kanagawa (JP)

(72) Inventor: **Tetsuya AOKI**, Kanagawa (JP)

(73) Assignee: **NISSAN MOTOR CO., LTD.**, Yokohama-shi, Kanagawa (JP)

(21) Appl. No.: **15/539,334**

(22) PCT Filed: **Dec. 26, 2014**

(86) PCT No.: **PCT/JP2014/084566**

§ 371 (c)(1),
(2) Date: **Jun. 23, 2017**

**Publication Classification**

(51) **Int. Cl.**

| | |
|---|---|
| ***H01M 8/04119*** | (2006.01) |
| ***H01M 8/0438*** | (2006.01) |
| ***H01M 8/04537*** | (2006.01) |

(52) **U.S. Cl.**

CPC ... ***H01M 8/04119*** (2013.01); ***H01M 8/04641*** (2013.01); ***H01M 8/04582*** (2013.01); ***H01M 8/04388*** (2013.01); ***H01M 8/04395*** (2013.01); ***H01M 8/04552*** (2013.01)

(57) **ABSTRACT**

A state detection device for a fuel cell for generating power upon receiving a supply of anode gas and cathode gas, including an impedance acquisition unit configured to acquire a high frequency impedance based on a frequency selected from a high frequency band and a low frequency impedance based on a frequency selected from a low frequency band, the high frequency band including a frequency band which shows responsiveness at least to a state quantity of an anode electrode, the low frequency band including a frequency band which shows responsiveness at least to a state quantity of a cathode electrode, and an internal state quantity estimation unit configured to estimate each of the state quantity of the anode electrode and the state quantity of the cathode electrode by combining the acquired high frequency impedance and low frequency impedance, the state quantity of the anode electrode and the state quantity of the cathode electrode serving as internal states of the fuel cell.

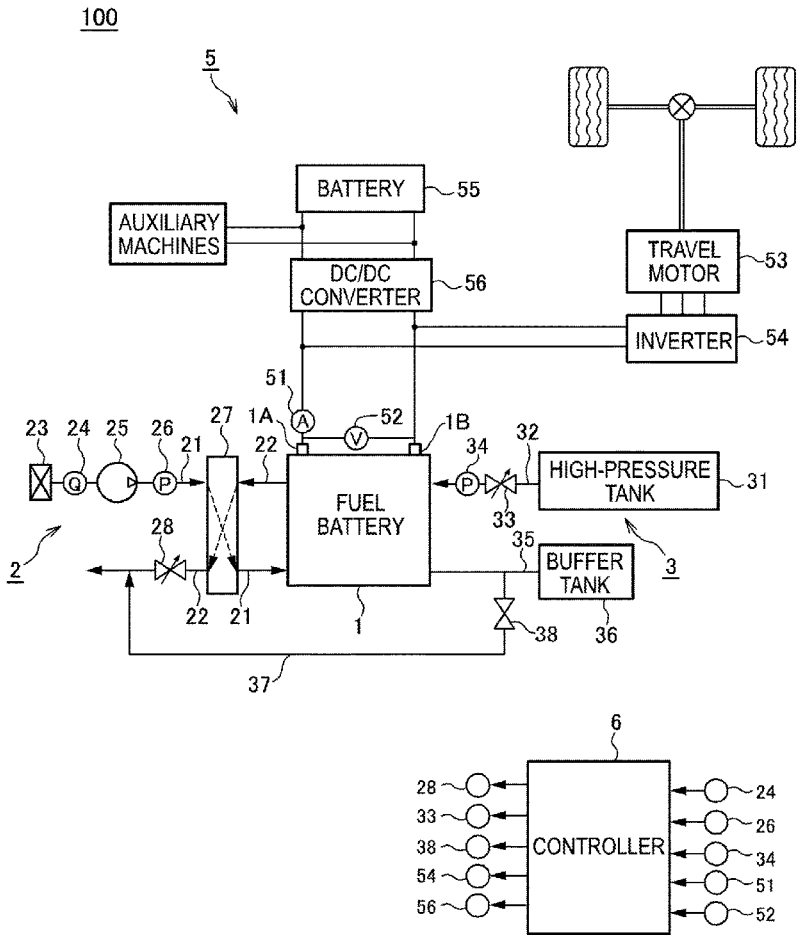

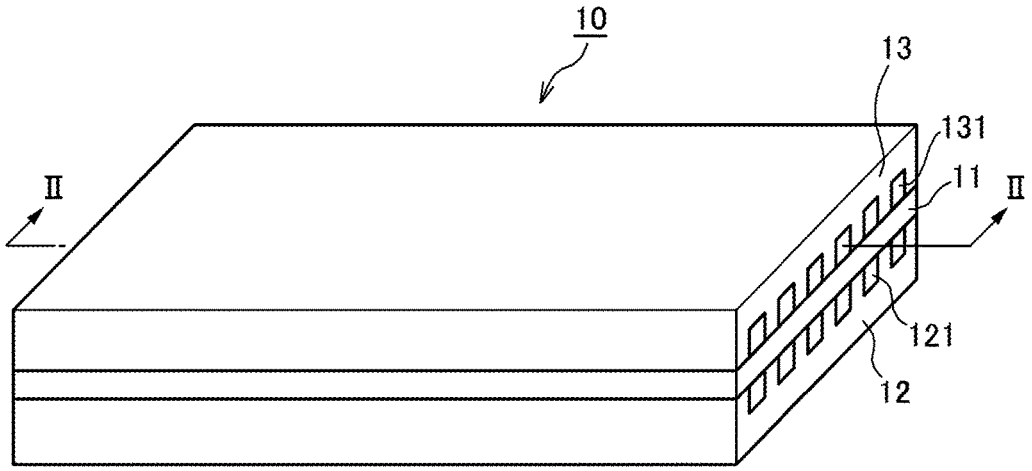


FIG.1

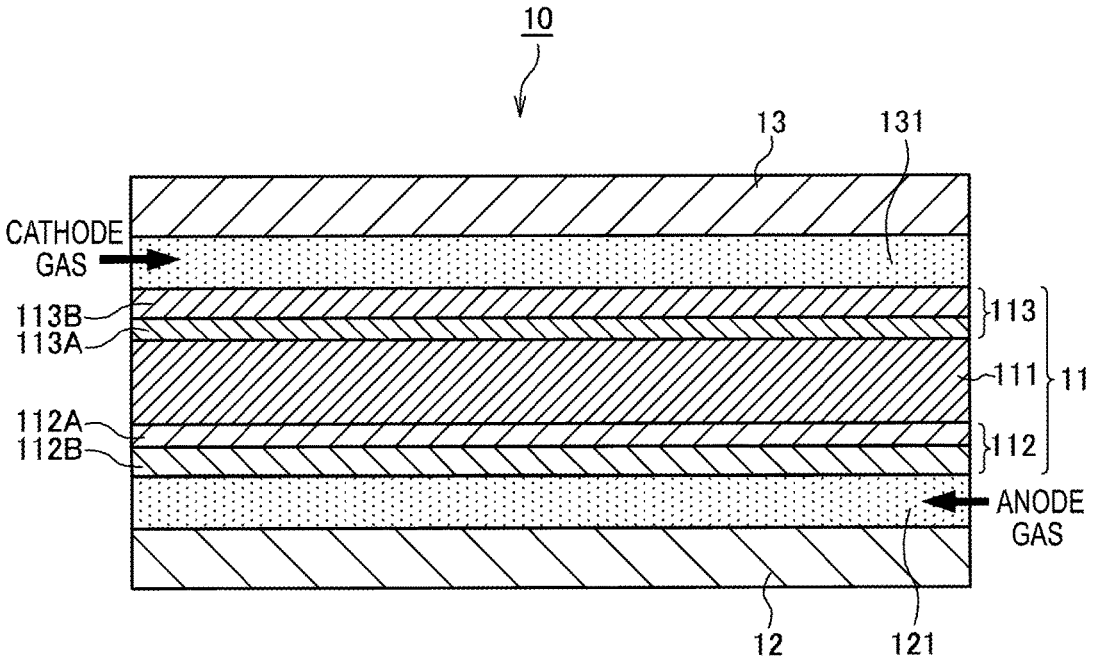
10
13
131
CATHODE GAS
113B
113A
112A
112B
113
111
11
112
ANODE GAS
12
121

FIG.2

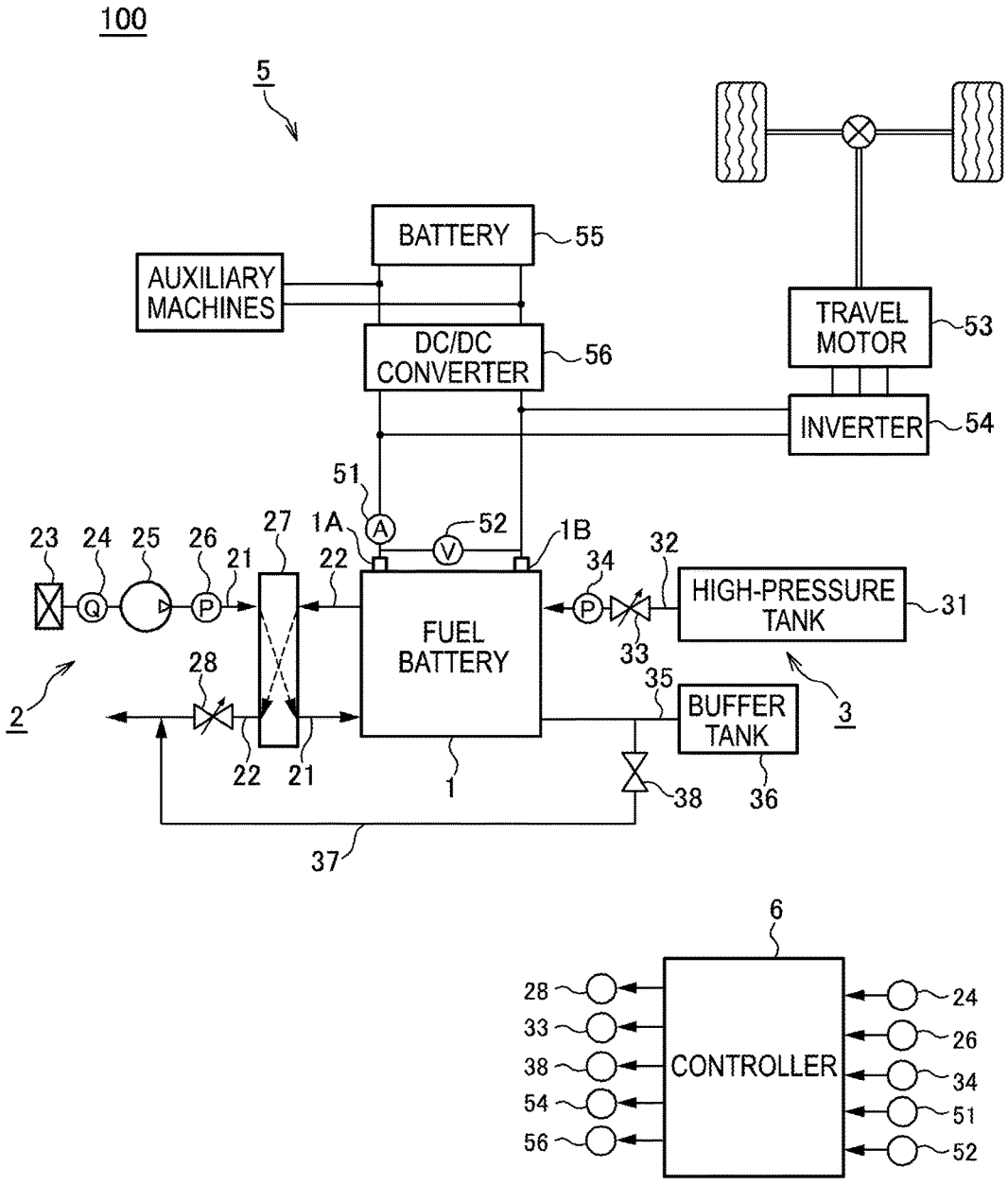
100
5
BATTERY
55
AUXILIARY MACHINES
DC/DC CONVERTER
56
TRAVEL MOTOR
53
INVERTER
54
51
52
23
24
25
26
21
27
1A
22
1B
32
34
HIGH-PRESSURE TANK
31
FUEL BATTERY
33
28
35
BUFFER TANK
2
3
22
21
1
38
36
37
6
CONTROLLER
28
33
38
54
56
24
26
34
51
52

FIG.3

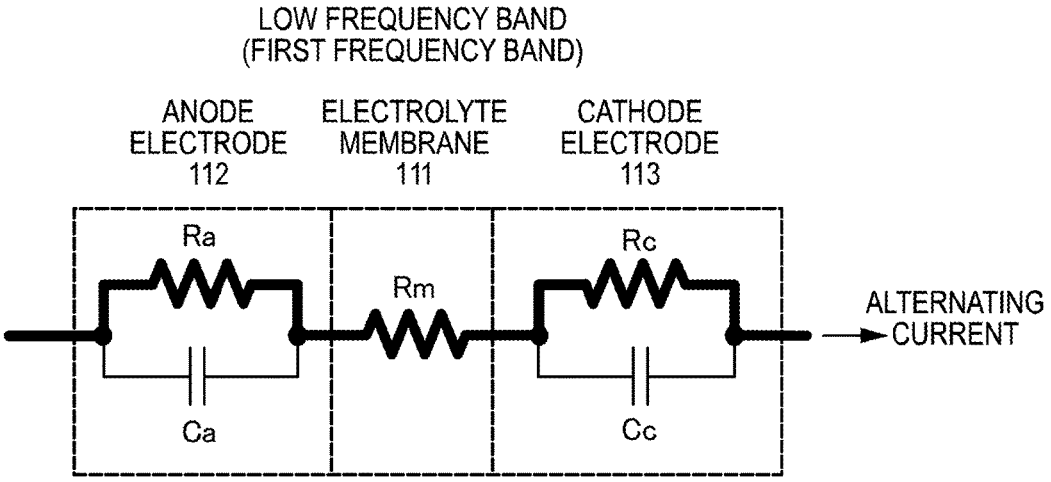
LOW FREQUENCY BAND
(FIRST FREQUENCY BAND)
ANODE ELECTRODE 112
ELECTROLYTE MEMBRANE 111
CATHODE ELECTRODE 113
Ra
Rm
Rc
Ca
Cc
ALTERNATING CURRENT

FIG.4A

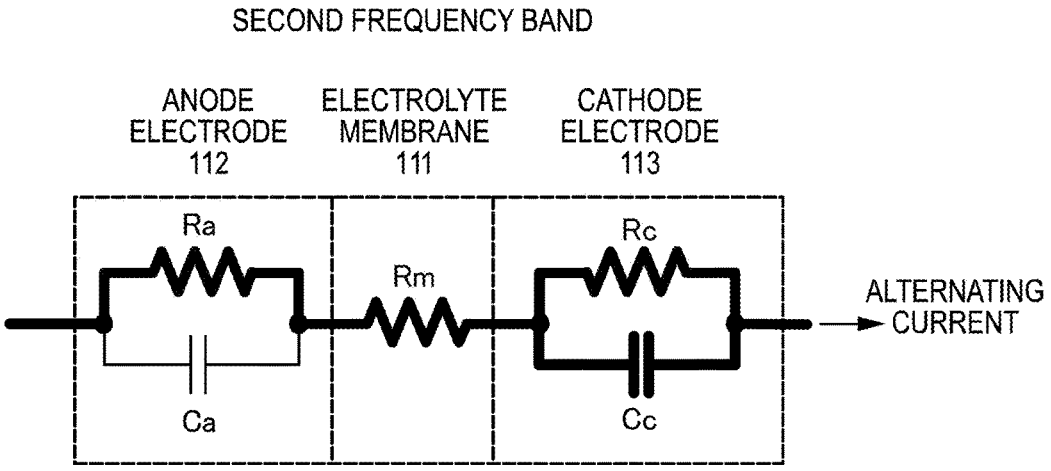
SECOND FREQUENCY BAND
ANODE ELECTRODE 112
ELECTROLYTE MEMBRANE 111
CATHODE ELECTRODE 113
Ra
Rm
Rc
Ca
Cc
ALTERNATING CURRENT

FIG.4B

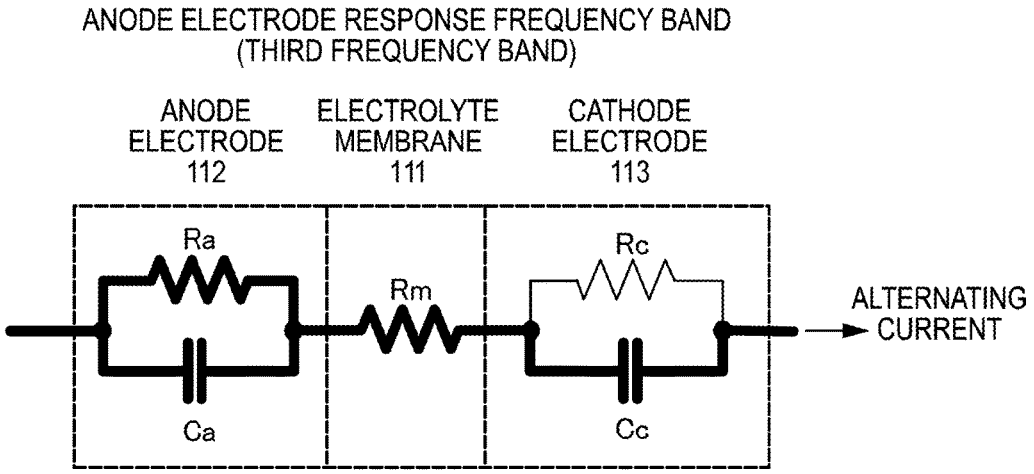
ANODE ELECTRODE RESPONSE FREQUENCY BAND
(THIRD FREQUENCY BAND)
ANODE ELECTRODE 112
ELECTROLYTE MEMBRANE 111
CATHODE ELECTRODE 113
Ra
Rm
Rc
Ca
Cc
ALTERNATING CURRENT

FIG.4C

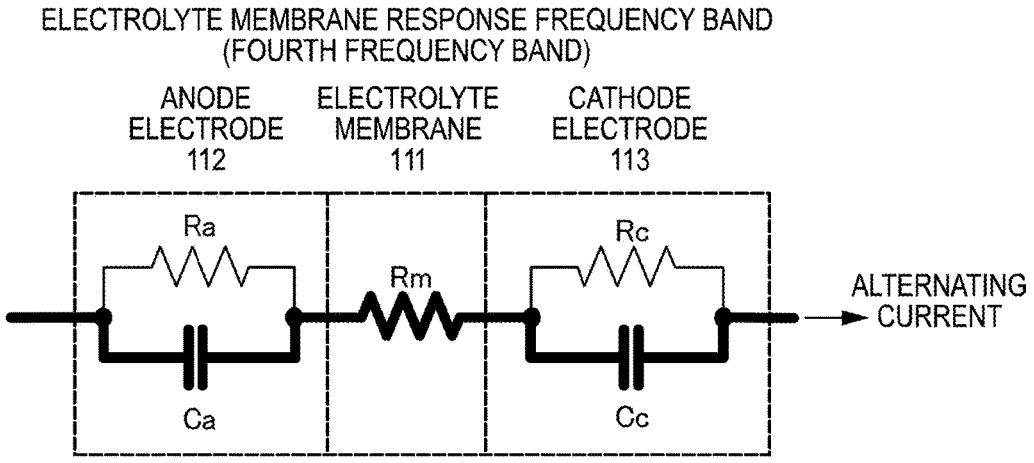
ELECTROLYTE MEMBRANE RESPONSE FREQUENCY BAND
(FOURTH FREQUENCY BAND)
ANODE ELECTRODE 112
ELECTROLYTE MEMBRANE 111
CATHODE ELECTRODE 113
Ra
Rm
Rc
Ca
Cc
ALTERNATING CURRENT

FIG.4D

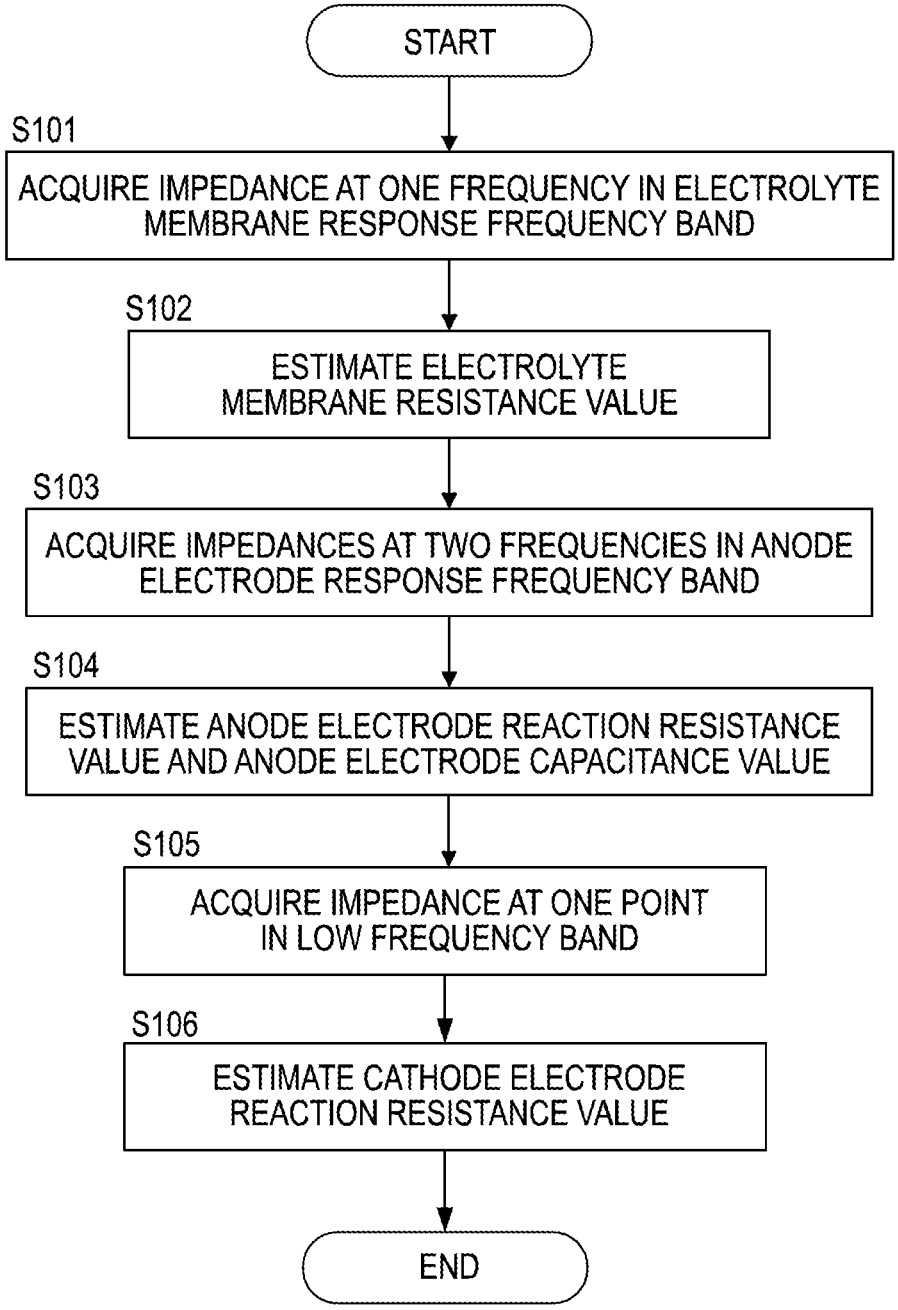
START
S101
ACQUIRE IMPEDANCE AT ONE FREQUENCY IN ELECTROLYTE MEMBRANE RESPONSE FREQUENCY BAND
S102
ESTIMATE ELECTROLYTE MEMBRANE RESISTANCE VALUE
S103
ACQUIRE IMPEDANCES AT TWO FREQUENCIES IN ANODE ELECTRODE RESPONSE FREQUENCY BAND
S104
ESTIMATE ANODE ELECTRODE REACTION RESISTANCE VALUE AND ANODE ELECTRODE CAPACITANCE VALUE
S105
ACQUIRE IMPEDANCE AT ONE POINT IN LOW FREQUENCY BAND
S106
ESTIMATE CATHODE ELECTRODE REACTION RESISTANCE VALUE
END

FIG.5

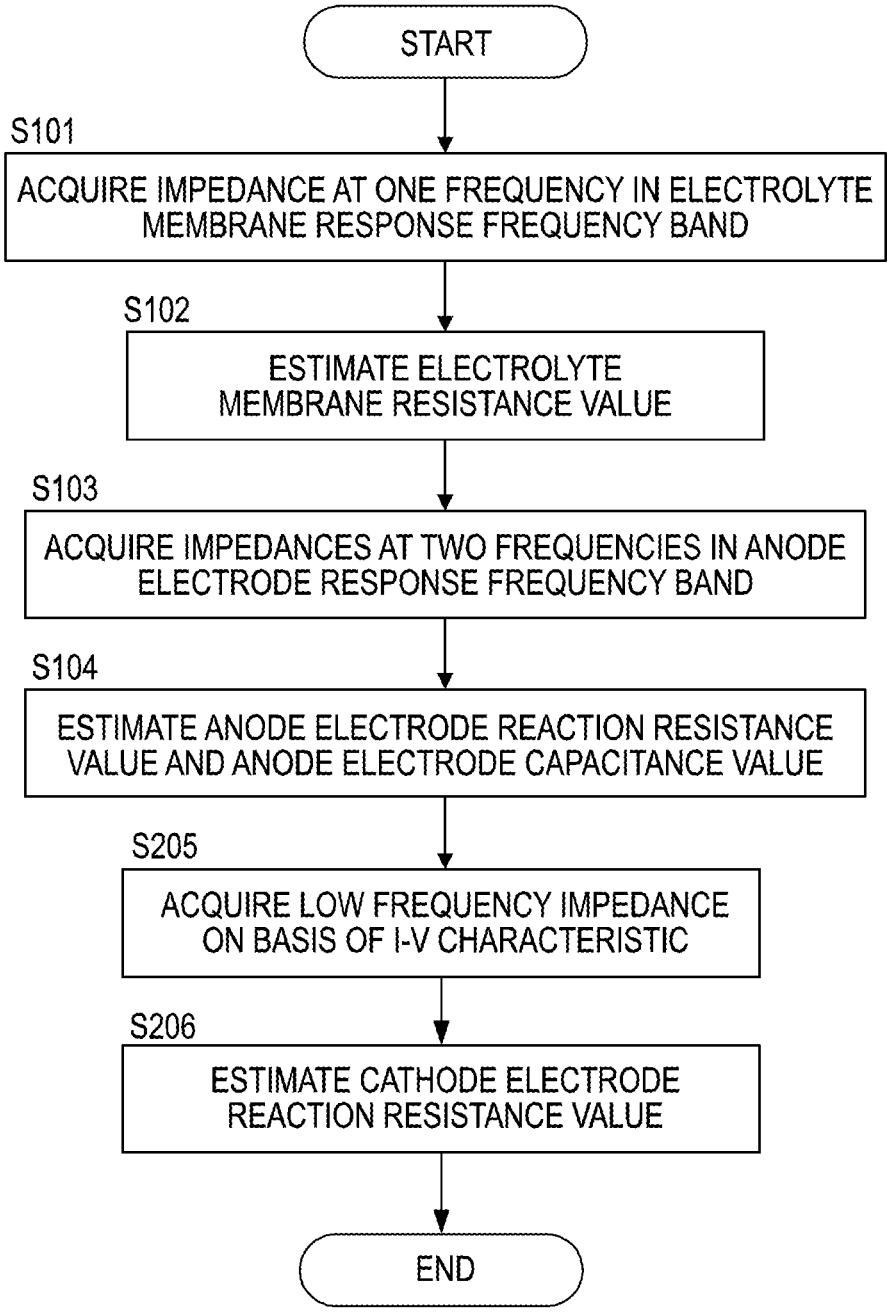
START
S101
ACQUIRE IMPEDANCE AT ONE FREQUENCY IN ELECTROLYTE MEMBRANE RESPONSE FREQUENCY BAND
S102
ESTIMATE ELECTROLYTE MEMBRANE RESISTANCE VALUE
S103
ACQUIRE IMPEDANCES AT TWO FREQUENCIES IN ANODE ELECTRODE RESPONSE FREQUENCY BAND
S104
ESTIMATE ANODE ELECTRODE REACTION RESISTANCE VALUE AND ANODE ELECTRODE CAPACITANCE VALUE
S205
ACQUIRE LOW FREQUENCY IMPEDANCE ON BASIS OF I-V CHARACTERISTIC
S206
ESTIMATE CATHODE ELECTRODE REACTION RESISTANCE VALUE
END

FIG.6

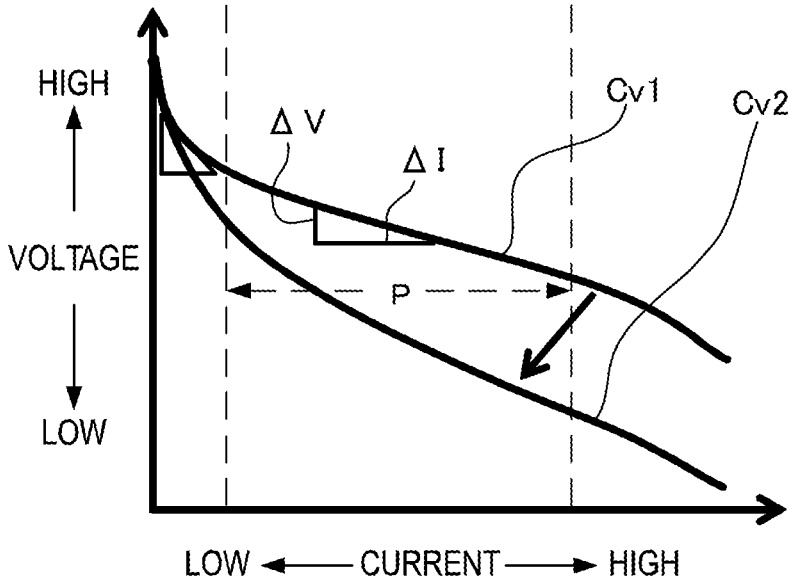


FIG.7

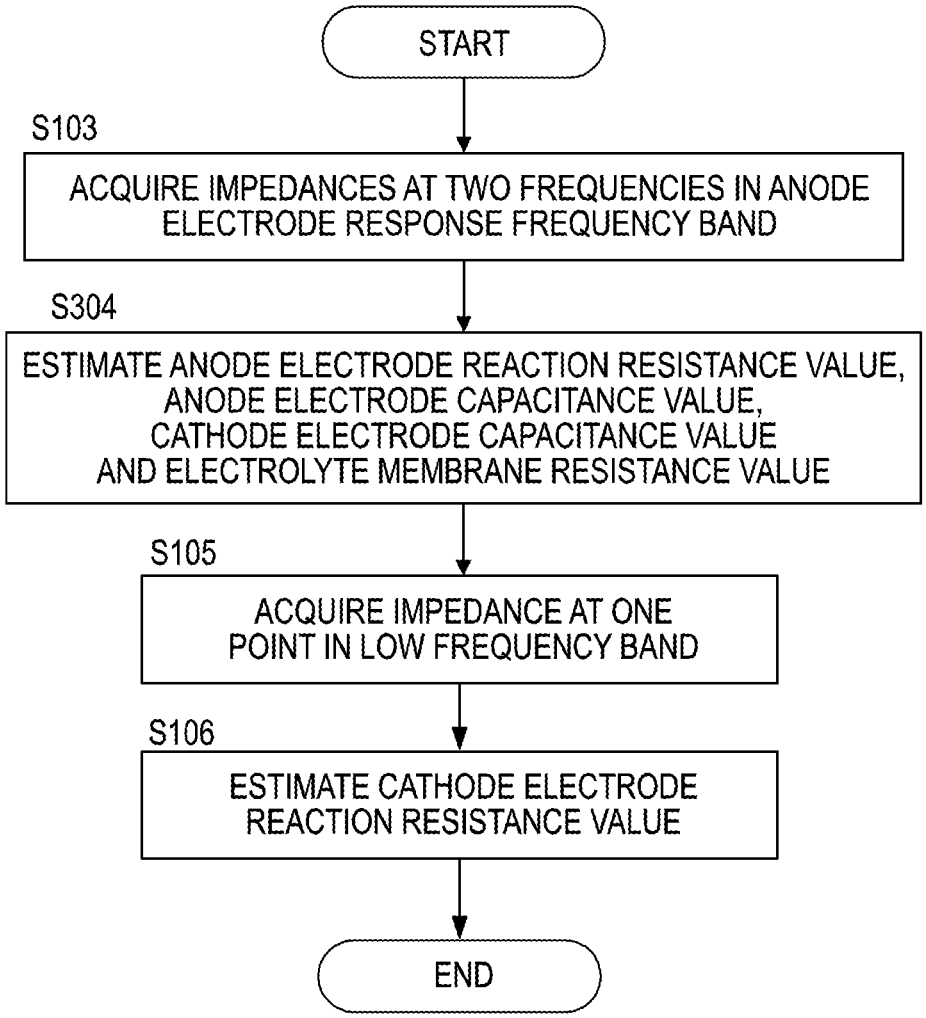
START
S103
ACQUIRE IMPEDANCES AT TWO FREQUENCIES IN ANODE ELECTRODE RESPONSE FREQUENCY BAND
S304
ESTIMATE ANODE ELECTRODE REACTION RESISTANCE VALUE, ANODE ELECTRODE CAPACITANCE VALUE, CATHODE ELECTRODE CAPACITANCE VALUE AND ELECTROLYTE MEMBRANE RESISTANCE VALUE
S105
ACQUIRE IMPEDANCE AT ONE POINT IN LOW FREQUENCY BAND
S106
ESTIMATE CATHODE ELECTRODE REACTION RESISTANCE VALUE
END

FIG.8

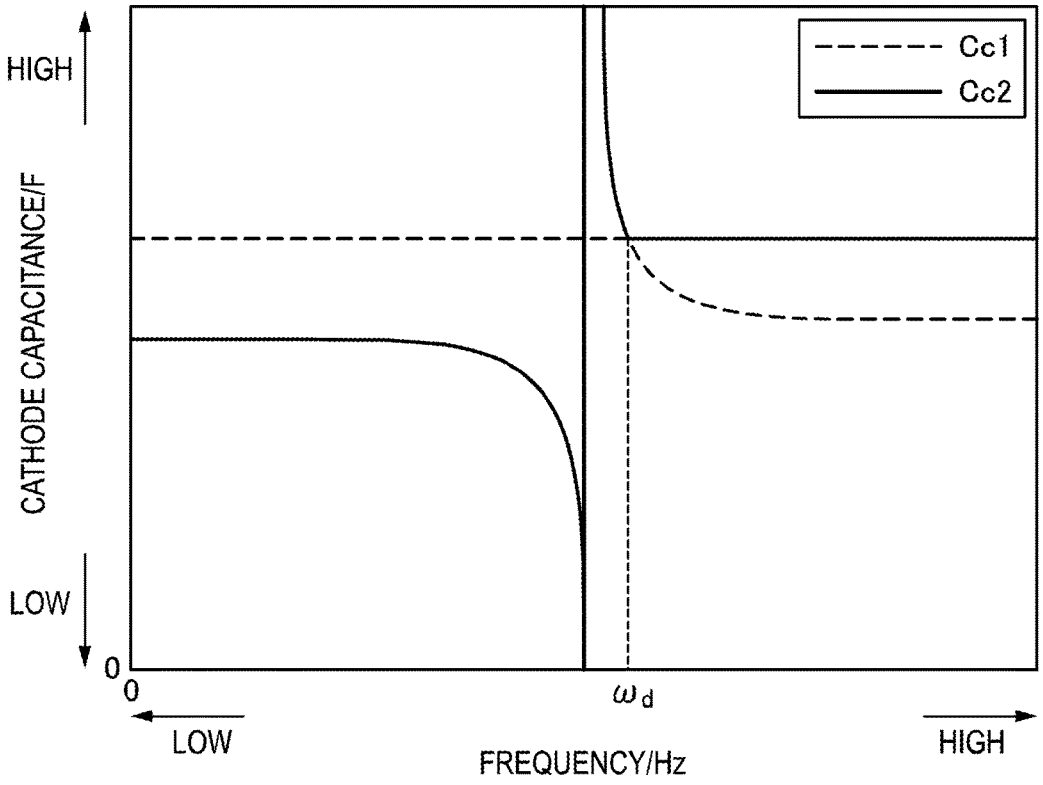
HIGH
CATHODE CAPACITANCE/F
LOW
0
0
Cc1
Cc2
ωd
LOW
FREQUENCY/Hz
HIGH

FIG.9

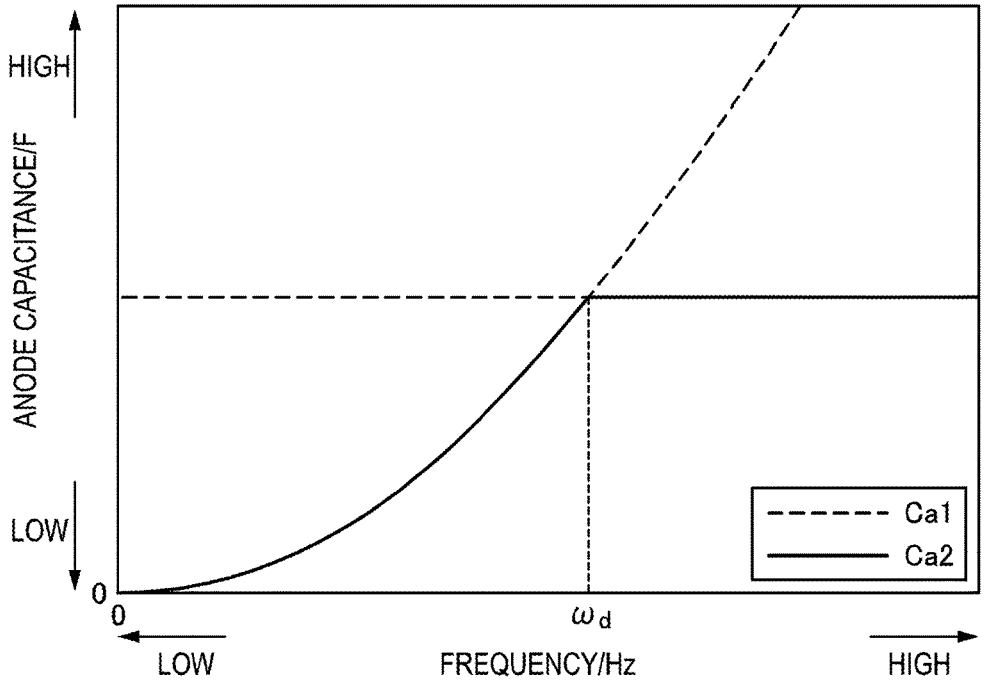


FIG.10A

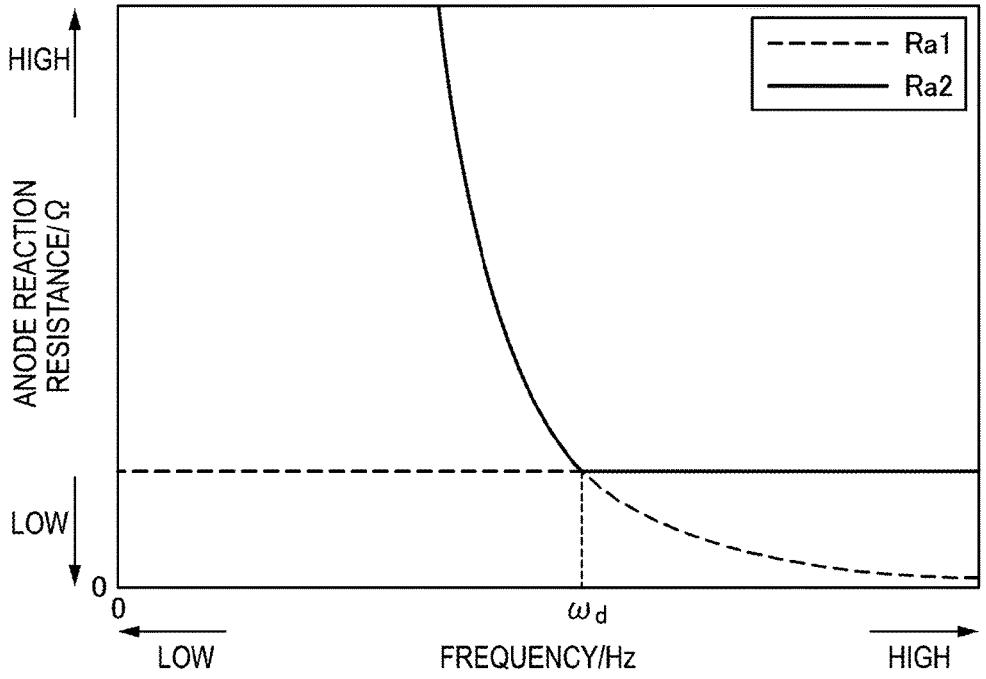


FIG.10B

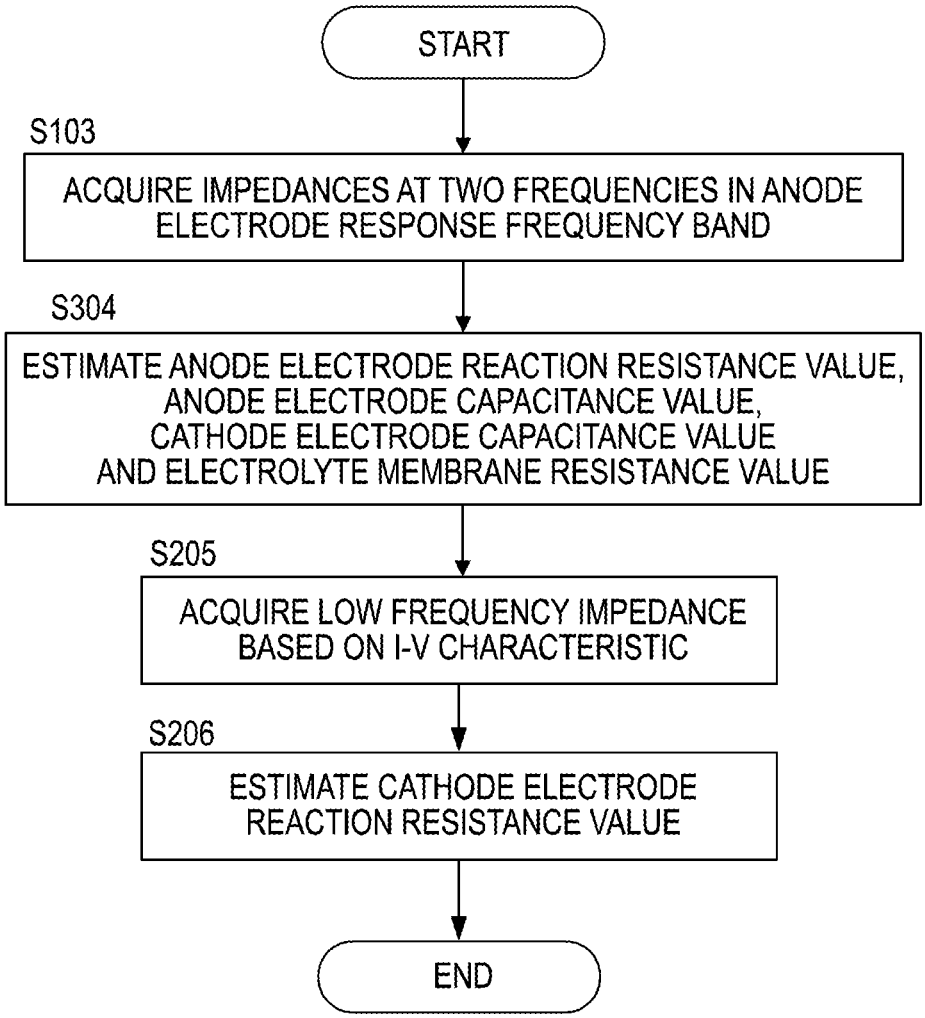
START
S103
ACQUIRE IMPEDANCES AT TWO FREQUENCIES IN ANODE ELECTRODE RESPONSE FREQUENCY BAND
S304
ESTIMATE ANODE ELECTRODE REACTION RESISTANCE VALUE, ANODE ELECTRODE CAPACITANCE VALUE, CATHODE ELECTRODE CAPACITANCE VALUE AND ELECTROLYTE MEMBRANE RESISTANCE VALUE
S205
ACQUIRE LOW FREQUENCY IMPEDANCE BASED ON I-V CHARACTERISTIC
S206
ESTIMATE CATHODE ELECTRODE REACTION RESISTANCE VALUE
END

FIG.11

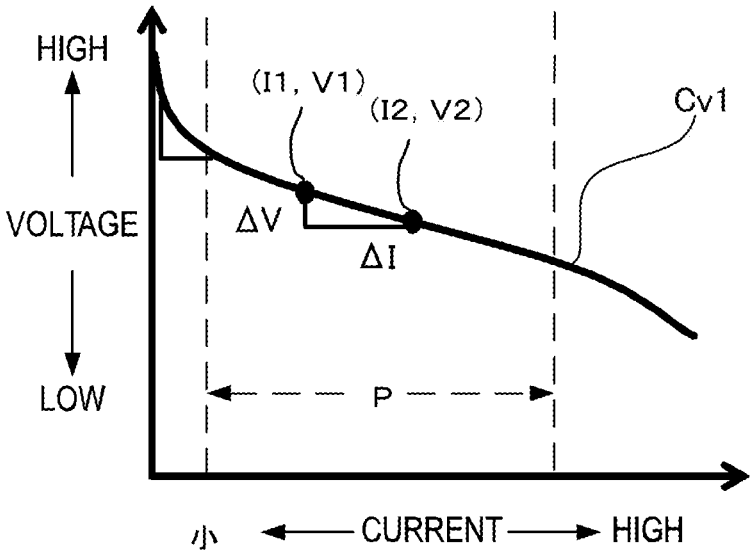


FIG.12

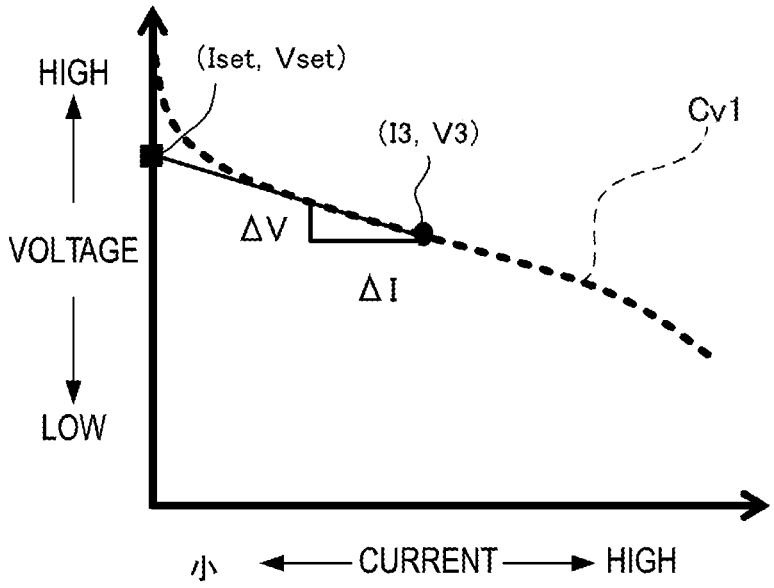


FIG.13

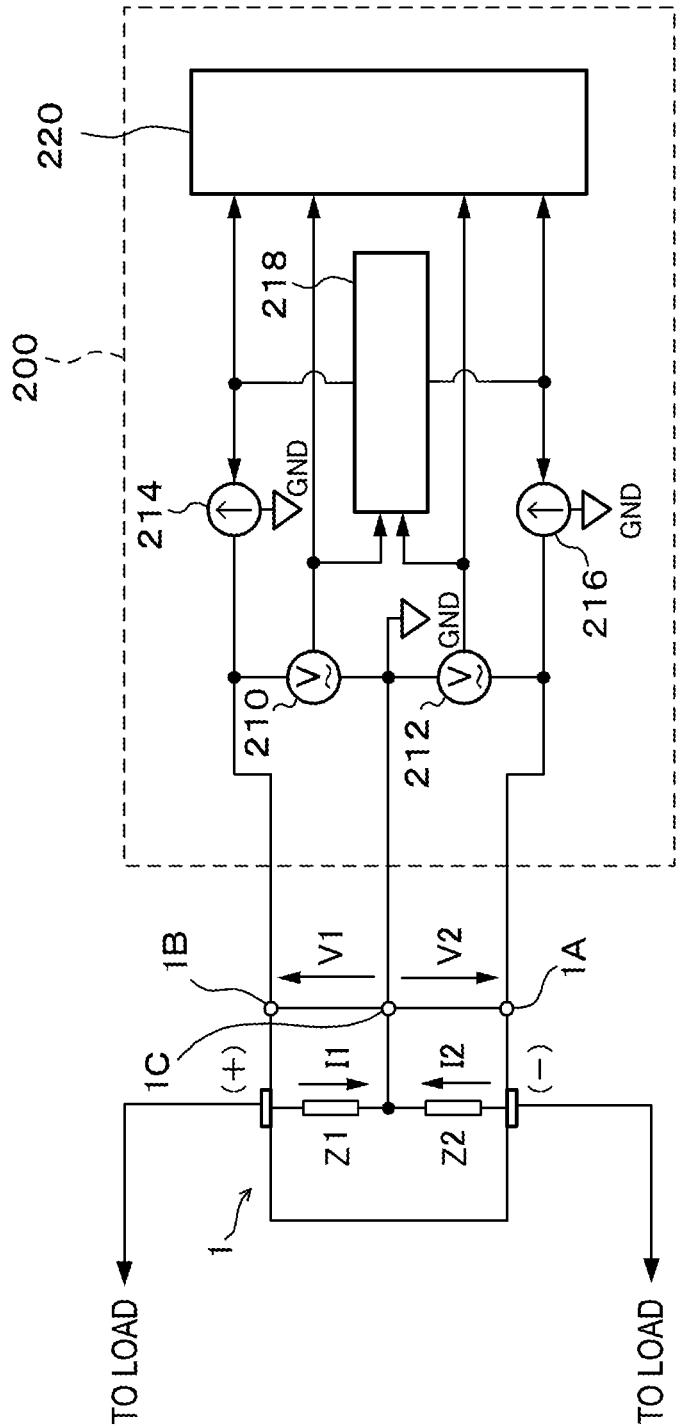
220
200
218
214
GND
216
GND
GND
210
212
1B
V1
V2
1A
1C
(+)
I1
I2
(−)
Z1
Z2
1
TO LOAD
TO LOAD

FIG.14

# STATE DETECTION DEVICE AND METHOD FOR FUEL CELL

## TECHNICAL FIELD

**[0001]** This invention relates to state detection device and method for fuel cell.

## BACKGROUND ART

**[0002]** A state detection device for fuel cell is known which measures a voltage value and an impedance value of a fuel cell and detects an internal state of the fuel cell on the basis of these values.

**[0003]** For example, it is proposed in Japanese Patent No. 4640661 to calculate a first impedance in a first frequency region corresponding to an electrolyte membrane resistance and a second impedance in a second frequency region corresponding to the sum of the electrolyte membrane resistance and a catalyst layer resistance and lower than the first frequency region and calculate a water content of a catalyst layer on the basis of a differential impedance between the second and first impedances.

**[0004]** Further, it is described in JP2005-285614A to acquire complex impedances corresponding to a frequency $F_1$ at an intersection with a real axis of a complex impedance curve (Cole-Cole plot) of a fuel cell, a frequency $F_2$ in a first region expressing a reaction resistance (reaction resistance of a cathode electrode) when oxygen reacts and a frequency $F_3$ in a second region expressing a resistance concerning oxygen diffusion and obtain an internal resistance value from the obtained complex impedances.

## SUMMARY OF INVENTION

**[0005]** However, it is not possible to grasp each of state quantities of an anode electrode and those of a cathode electrode in Japanese Patent No. 4640661. Further, it is also difficult in JP2005-285614A to individually grasp the state of the anode electrode and that of the cathode electrode since the state of the anode electrode and that of the cathode electrode are mixed in the impedance curve.

**[0006]** The present invention was developed, focusing on such a problem, and aims to provide a state detection device and method for fuel cell capable of individually detecting internal state quantities such as state quantities of an anode electrode and those of a cathode electrode in a fuel cell.

**[0007]** According to one aspect of the present invention, the present invention provides a state detection device for a fuel cell for generating power upon receiving a supply of anode gas and cathode gas. More specifically, the state detection device includes an impedance acquisition unit configured to acquire a high frequency impedance based on a frequency selected from a high frequency band and a low frequency impedance based on a frequency selected from a low frequency band, the high frequency band including a frequency band which shows responsiveness at least to a state quantity of an anode electrode, the low frequency band including a frequency band which shows responsiveness at least to a state quantity of a cathode electrode, and an internal state quantity estimation unit configured to estimate each of the state quantity of the anode electrode and the state quantity of the cathode electrode by combining the acquired high frequency impedance and low frequency impedance, the state quantity of the anode electrode and the state quantity of the cathode electrode serving as internal states of the fuel cell.

## BRIEF DESCRIPTION OF DRAWINGS

**[0008]** FIG. **1** is a perspective view of a fuel cell according to an embodiment of the present invention,

**[0009]** FIG. **2** is a sectional view along II-II of the fuel cell of FIG. **1**,

**[0010]** FIG. **3** is a schematic configuration diagram of a fuel cell system according to the embodiment of the present invention.

**[0011]** FIG. **4**A is a diagram showing a path of a current flowing in a simplified equivalent circuit model of a fuel cell in the case of applying an alternating-current voltage in a low frequency band.

**[0012]** FIG. **4**B is a diagram showing a path of a current flowing in the simplified equivalent circuit model of the fuel cell in the case of applying an alternating-current voltage in a frequency band higher than in the case of FIG. **4**A.

**[0013]** FIG. **4**C is a diagram showing a path of a current flowing in the simplified equivalent circuit model of the fuel cell in the case of applying an alternating-current voltage in a frequency band higher than in the case of FIG. **4**B.

**[0014]** FIG. **4**D is a diagram showing a path of a current flowing in the simplified equivalent circuit model of the fuel cell in the case of inputting an alternating-current voltage in a high frequency band.

**[0015]** FIG. **5** is a flow chart showing the flow of state quantity estimation according to one embodiment.

**[0016]** FIG. **6** is a flow chart showing the flow of state quantity estimation according to one embodiment.

**[0017]** FIG. **7** is a graph showing I-V characteristic curves of the fuel cell respectively in steady time and in unsteady time.

**[0018]** FIG. **8** is a flow chart showing the flow of state quantity estimation according to one embodiment.

**[0019]** FIG. **9** shows frequency responses of candidates for an electrical double layer capacitance of a cathode electrode.

**[0020]** FIG. **10**A shows frequency responses of candidates for an electrical double layer capacitance of an anode electrode.

**[0021]** FIG. **10**B shows frequency responses of candidates for a reaction resistance value of the anode electrode **112**.

**[0022]** FIG. **11** is a flow chart showing the flow of state quantity estimation according to one embodiment.

**[0023]** FIG. **12** shows an I-V characteristic curve of the fuel cell **1** in steady time,

**[0024]** FIG. **13** is a graph showing an example of a method for setting a set of current and voltage for the calculation of a gradient $\Delta V/\Delta I$ in the I-V characteristic curve, and

**[0025]** FIG. **14** is a block diagram schematically showing a main part relating to an impedance measurement in a fuel cell system according to one embodiment.

## DESCRIPTION OF EMBODIMENTS

**[0026]** Hereinafter, embodiments of the present invention are described with reference to the drawings and the like.

**[0027]** A fuel cell is configured such that an electrolyte membrane is sandwiched by an anode electrode serving as a fuel electrode and a cathode electrode serving as an oxidant electrode. The fuel cell generates power using anode

gas containing hydrogen and supplied to the anode electrode and cathode gas containing oxygen and supplied to the cathode electrode. Electrode reactions which proceed in both anode and cathode electrodes are as follows.

$$\text{Anode electrode: } 2H_2 \rightarrow 4H^+ + 4e^- \quad (1)$$

$$\text{Cathode electrode: } 4H^+ + 4e^- + O_2 \rightarrow 2H_2O \quad (2)$$

**[0028]** FIGS. **1** and **2** are views showing the configuration of a fuel cell **10** according to one embodiment of the present invention. FIG. **1** is a perspective view of the fuel cell **10**. FIG. **2** is a sectional view along II-II of the fuel cell **10** of FIG. **1**.

**[0029]** As shown in FIGS. **1** and **2**, the fuel cell **10** includes a membrane electrode assembly (MEA) **11**, and an anode separator **12** and a cathode separator **13** arranged to sandwich the MEA **11**.

**[0030]** The MEA **11** is composed of an electrolyte membrane **111**, an anode electrode **112** and a cathode electrode **113**. The MEA **11** includes the anode electrode **112** on one surface side of the electrolyte membrane **111** and the cathode electrode **113** on the other surface side.

**[0031]** The electrolyte membrane **11** is a proton conductive ion exchange membrane formed of fluororesin. The electrolyte membrane **111** exhibits good electrical conductivity in a wet state. It should be noted that another material such as a material having a phosphoric acid ($H_3PO_4$) impregnated in a predetermined matrix may be used according to a possible response of a fuel cell.

**[0032]** The anode electrode **112** includes a catalyst layer **112**A and a gas diffusion layer **112**B. The catalyst layer **112**A is a member formed of platinum or carbon black particles carrying platinum or the like and provided in contact with the electrolyte membrane **111**. The gas diffusion layer **112**B is provided on an outer side of the catalyst layer **112**A. The gas diffusion layer **112**B is a member formed of carbon cloth having gas diffusion property and electrical conductivity and provided in contact with the catalyst layer **112**A and the anode separator **12**.

**[0033]** Similarly to the anode electrode **112**, the cathode electrode **13** also includes a catalyst layer **113**A and a gas diffusion layer **113**B. The catalyst layer **113**A is arranged between the electrolyte membrane **111** and the gas diffusion layer **113**B and the gas diffusion layer **113**B is arranged between the catalyst layer **113**A and the cathode separator **13**.

**[0034]** The anode separator **112** is arranged on an outer side of the gas diffusion layer **112**B. The anode separator **12** includes a plurality of anode gas flow passages **121** for supplying anode gas (hydrogen gas) to the anode electrode **112**. The anode gas flow passages **121** are formed as groove-like passages.

**[0035]** The cathode separator **13** is arranged on an outer side of the gas diffusion layer **113**B. The cathode separator **13** includes a plurality of cathode gas flow passages **131** for supplying cathode gas (air) to the cathode electrode **113**. The cathode gas flow passages **131** are formed as groove-like passages.

**[0036]** The anode separator **12** and the cathode separator **13** are so configured that the anode gas flowing in the anode gas flow passages **121** and the cathode gas flowing in the cathode gas flow passages **131** flow in directions opposite to each other. It should be noted that the anode separator **12** and the cathode separator **13** may be so configured that these gases flow in the same direction.

**[0037]** In the case of using such a fuel cell **10** as a power source for an automotive vehicle, a fuel cell stack in which several hundreds of fuel cells **10** are laminated is used since required power is large. Power for driving the vehicle is taken out by configuring a fuel cell system for supplying anode gas and cathode gas to the fuel cell stack. It should be noted that although an impedance measurement to be described later is conducted for each fuel cell stack in which the fuel cells **10** are laminated in the present embodiment, the impedance measurement may be conducted for each fuel cell **10** or for each part (e.g., several tens of cells) of the fuel cell stack.

**[0038]** Further, in the fuel cell stack, an anode electrode, a cathode electrode and an electrolyte membrane serving as sums are configured by arranging the anode electrodes **112**, the cathode electrodes **113** and the electrolyte membranes **111** of a plurality of the fuel cells **10** in series. However, for the convenience of description, these anode electrode, cathode electrode and electrolyte membrane serving as the sums are also denoted by the same reference signs as the anode electrode **112**, the cathode electrode **113** and the electrolyte membrane **111** of the single cell.

**[0039]** FIG. **3** is a schematic diagram of a fuel cell system **100** according to one embodiment of the present invention.

**[0040]** The fuel cell system **100** includes a fuel cell **1**, a cathode gas supplying/discharging device **2**, an anode gas supplying/discharging device **3**, a power system **5** and a controller **6**.

**[0041]** The fuel cell **1** is a laminated battery formed by laminating a plurality of fuel cells **10** (unit cells) as described above. The fuel cell **1** generates power necessary to drive a vehicle upon receiving the supply of the anode gas and the cathode gas. The fuel cell **1** includes an anode electrode side terminal **1**A and a cathode electrode side terminal **1**B as output terminals for taking out power.

**[0042]** The cathode gas supplying/discharging device **2** supplies the cathode gas to the fuel cell **1** and discharges cathode off-gas discharged from the fuel cell **1** to outside. The cathode gas supplying/discharging device **2** includes a cathode gas supply passage **21**, a cathode gas discharge passage **22**, a filter **23**, an air flow sensor **24**, a cathode compressor **25**, a cathode pressure sensor **26**, a water recovery device (WRD) **27** and a cathode pressure control valve **28**.

**[0043]** The cathode gas supply passage **21** is a passage in which the cathode gas to be supplied to the fuel cell **1** flows. One end of the cathode gas supply passage **21** is connected to the filter **23** and the other end is connected to a cathode gas inlet part of the fuel cell **1**.

**[0044]** The cathode gas discharge passage **22** is a passage in which the cathode off-gas discharged from the fuel cell **1** flows. One end of the cathode gas discharge passage **22** is connected to a cathode gas outlet part of the fuel cell **1** and the other end is formed as an opening end. The cathode off-gas is mixture gas containing the cathode gas, steam produced by the electrode reaction and the like.

**[0045]** The filter **23** is a member for removing dust, dirt and the like contained in the cathode gas to be taken into the cathode gas supply passage **21**.

**[0046]** The cathode compressor **25** is provided downstream of the filter **23** in the cathode gas supply passage **21**. The cathode compressor **25** supplies the cathode gas in the cathode gas supply passage **21** to the fuel cell **1** by feeding the cathode gas under pressure.

**[0047]** The air flow sensor **24** is provided between the filter **23** and the cathode compressor **25** in the cathode gas supply passage **21**. The air flow sensor **24** detects a flow rate of the cathode gas to be supplied to the fuel cell **1**.

**[0048]** The cathode pressure sensor **26** is provided between the cathode compressor **25** and the WRD **27** in the cathode gas supply passage **21**. The cathode pressure sensor **26** detects a pressure of the cathode gas to be supplied to the fuel cell **1**. The cathode gas pressure detected by the cathode pressure sensor **26** represents a pressure of an entire cathode system including the cathode gas flow passages of the fuel cell **1** and the like.

**[0049]** The WRD **27** is connected over the cathode gas supply passage **21** and the cathode gas discharge passage **22**. The WRD **27** is a device for recovering moisture in the cathode off-gas flowing in the cathode gas discharge passage **22** and humidifying the cathode gas flowing in the cathode gas supply passage **21** with that recovered moisture.

**[0050]** The cathode pressure control valve **28** is provided downstream of the WRD **27** in the cathode gas discharge passage **22**. The cathode pressure control valve **28** is controlled to open and close by the controller **6** and adjusts the pressure of the cathode gas to be supplied to the fuel cell **1**.

**[0051]** Next, the anode gas supplying/discharging device **3** is described.

**[0052]** The anode gas supplying/discharging device **3** supplies the anode gas to the fuel cell **1** and discharges anode off-gas discharged from the fuel cell to the cathode gas discharge passage **22**. The anode gas supplying/discharging device **3** includes a high-pressure tank **31**, an anode gas supply passage **32**, an anode pressure control valve **33**, an anode pressure sensor **34**, an anode gas discharge passage **35**, a buffer tank **36**, a purge passage **37** and a purge valve **38**.

**[0053]** The high-pressure tank **31** is a container for storing the anode gas to be supplied to the fuel cell **1** in a high-pressure state.

**[0054]** The anode gas supply passage **32** is a passage for supplying the anode gas discharged from the high-pressure tank **31** to the fuel cell **1**. One end of the anode gas supply passage **32** is connected to the high-pressure tank **31** and the other end is connected to an anode gas inlet part of the fuel cell **1**.

**[0055]** The anode pressure control valve **33** is provided downstream of the high-pressure tank **31** in the anode gas supply passage **32**. The anode pressure control valve **33** is controlled to open and close by the controller **6** and adjusts the pressure of the anode gas to be supplied to the fuel cell **1**.

**[0056]** The anode pressure sensor **34** is provided downstream of the anode pressure control valve **33** in the anode gas supply passage **32**. The anode pressure sensor **34** detects a pressure of the anode gas to be supplied to the fuel cell **1**. The anode gas pressure detected by the anode pressure sensor **34** represents a pressure of an entire anode system including the buffer tank **36**, the anode gas flow passages of the fuel cell **1** and the like.

**[0057]** The anode gas discharge passage **35** is a passage in which the anode off-gas discharged from the fuel cell **1** flows. One end of the anode gas discharge passage **35** is connected to an anode gas outlet part of the fuel cell **1** and the other end is connected to the buffer tank **36**. The anode off-gas contains the anode gas not used in the electrode reaction, impurity gas such as nitrogen having leaked from the cathode gas flow passages **131** to the anode gas flow passages **121**, moisture and the like.

**[0058]** The buffer tank **36** is a container for temporarily storing the anode off-gas flowing from the anode gas discharge passage **35**. The anode off-gas pooled in the buffer tank **36** is discharged to the cathode gas discharge passage **22** through the purge passage **37** when the purge valve **38** is opened.

**[0059]** The purge passage **37** is a passage for discharging the anode off-gas. One end of the purge passage **37** is connected to the anode gas discharge passage **35** and the other end is connected to a part of the cathode gas discharge passage **22** downstream of the cathode pressure control valve **28**.

**[0060]** The purge valve **38** is provided in the purge passage **37**. The purge valve **38** is controlled to open and close by the controller **6** and controls a purge flow rate of the anode off-gas discharged from the anode gas discharge passage **35** to the cathode gas discharge passage **22**.

**[0061]** When a purge control is executed to open the purge valve **38**, the anode off-gas is discharged to outside through the purge passage **37** and the cathode gas discharge passage **22**. At this time, the anode off-gas is mixed with the cathode off-gas in the cathode gas discharge passage **22**. By mixing the anode off-gas and the cathode off-gas and discharging the mixture gas to outside in this way, an anode gas concentration (hydrogen concentration) in the mixture gas is set at a value not larger than a discharge allowable concentration.

**[0062]** The power system **5** includes a current sensor **51**, a voltage sensor **52**, a travel motor **53**, an inverter **54**, a battery **55** and a DC/DC converter **56**.

**[0063]** The current sensor **51** detects an output current extracted from the fuel cell **1**. The voltage sensor **52** detects an output voltage of the fuel cell **1**, i.e., an inter-terminal voltage between the anode electrode side terminal **1**A and the cathode electrode side terminal **1**B. The voltage sensor **52** may be configured to detect a voltage of each fuel cell **10** or may be configured to detect a voltage of each group composed of a plurality of the fuel cells **10**.

**[0064]** The travel motor **53** is a three-phase alternating-current synchronous motor and a drive source for driving wheels. The travel motor **53** has a function serving as a motor to be rotationally driven upon receiving the supply of power from the fuel cell **1** and the battery **55** and a function serving as a generator for generating power by being rotationally driven by an external force.

**[0065]** The inverter **54** is composed of a plurality of semiconductor switches such as IGBTs. The semiconductor switches of the inverter **54** are switching-controlled by the controller **6**, thereby converting direct-current power into alternating-current power or alternating-current power into direct-current power. The inverter **54** converts composite direct-current power of output power of the fuel cell **1** and output power of the battery **55** into three-phase alternating-current power and supplies this power to the travel motor **53** when the travel motor **53** is caused to function as the motor. In contrast, the inverter **54** converts regenerative power (three-phase alternating-current power) of the travel motor **53** into direct-current power and supplies this power to the battery **55** when the travel motor **53** is caused to function as the generator.

**[0066]** The battery **55** is configured to be charged with a surplus of the output power of the fuel cell **1** and the

regenerative power of the travel motor **53**. The power charged into the battery **55** is supplied to the travel motor **53** and auxiliary machines such as the cathode compressor **25** if necessary.

**[0067]** The DC/DC converter **56** is a bidirectional voltage converter for increasing and decreasing the output voltage of the fuel cell **1**. By controlling the output voltage of the fuel cell **1** by the DC/DC converter **56**, the output current of the fuel cell **1** and the like are adjusted.

**[0068]** The controller **6** is configured by a microcomputer including a central processing unit (CPU), a read-only memory (ROM), a random access memory (RAM) and an input/output interface (I/O interface). To the controller **6** are input signals from sensors such as an accelerator stroke sensor (not shown) for detecting a depressed amount of an accelerator pedal besides signals from various sensors such as the current sensor **51** and the voltage sensor **52**.

**[0069]** The controller **6** adjusts the pressures and flow rates of the anode gas and the cathode gas to be supplied to the fuel cell **1** by controlling the anode pressure control valve **33**, the cathode pressure control valve **28**, the cathode compressor **25** and the like according to an operating state of the fuel cell system **100**.

**[0070]** Further, the controller **6** calculates target output power on the basis of power required by the travel motor **53**, power required by the auxiliary machines such as the cathode compressor **25**, charge/discharge requests of the battery **55** and the like. The controller **6** calculates a target output current of the fuel cell **1** on the basis of the target output power by referring to an IV characteristic (current-voltage characteristic) of the fuel cell **1** determined in advance. Then, the controller **6** controls the output voltage of the fuel cell **1** by the DC/DC converter **56** such that the output current of the fuel cell **1** reaches the target output current, and executes a control to supply a necessary current to the travel motor **53** and the auxiliary machines.

**[0071]** Further, the controller **6** controls the cathode compressor **25** and the like such that a degree of wetness (water content) of each electrolyte membrane **111** of the fuel cell **1** is in a state suitable for power generation.

**[0072]** Further, the controller calculates an impedance Z of the fuel cell **1** at a predetermined frequency by dividing an amplitude value of a voltage value, in which an alternating-current signal of the predetermined frequency is superimposed on an output voltage of the fuel cell **1**, by an amplitude value of a current value likewise superimposed with an alternating-current signal in first to sixth embodiments described later.

**[0073]** In the fuel cell system **100** described as above, a state detection device for the fuel cell **1** is configured by the controller **6**, the current sensor **51**, the voltage sensor **52** and the DC/DC converter **56**.

**[0074]** In the present embodiment, a simplified equivalent circuit model taking into account of a reaction resistance $R_a$ and an electrical double layer capacitance $C_a$, which are state quantities of the anode electrode **112** in the fuel cell **1**, a reaction resistance $R_c$ and an electrical double layer capacitance $C_c$, which are state quantities of the cathode electrode **113**, and an electrolyte membrane resistance value $R_m$, which is a state quantity of the electrolyte membrane **111**, is set and a state of the fuel cell **1** is estimated on the basis of this simplified equivalent circuit model.

**[0075]** It should be noted that the electrolyte membrane resistance value $R_m$ is a state quantity whose value is determined according to a degree of wetness of the electrolyte membrane **111**. Normally, as the electrolyte membrane **111** becomes drier, the electrolyte membrane resistance value $R_m$ tends to increase.

**[0076]** Further, the reaction resistance value $R_a$ of the anode electrode **112** increases and decreases according to the reaction of the anode gas in the anode electrode **112**. For example, if there is a factor due to which the reaction does not smoothly proceed such as a shortage of the anode gas, the reaction resistance value $R_a$ increases according to this.

**[0077]** Furthermore, the electrical double layer capacitance $C_a$ of the anode electrode **112** is modeled to represent an electrical capacitance of the anode electrode **112** in the fuel cell **1**. Thus, the electrical double layer capacitance $C_a$ is determined on the basis of various elements such as a constituting material, the size and the like of the anode electrode **112**.

**[0078]** Further, the reaction resistance value $R_c$ of the cathode electrode **113** increases and decreases according to the reaction of the cathode gas in the cathode electrode **113**. For example, if there is a factor due to which the reaction does not smoothly proceed such as a shortage of the cathode gas, the reaction resistance value $R_c$ increases according to this.

**[0079]** Furthermore, the electrical double layer capacitance $C_c$ of the cathode electrode **113** is modeled to represent an electrical capacitance of the cathode electrode **113**. Thus, the electrical double layer capacitance value $C_c$ is determined on the basis of various elements such as a constituting material, the size and the like of the cathode electrode **113**.

**[0080]** Here, the present inventors found out that there was a frequency dependent characteristic in a path, along which an alternating-current signal (alternating current) superimposed on an output current of the fuel cell **1** flowed in the fuel cell, in the simplified equivalent circuit model of the fuel cell **1**. The frequency dependent characteristic in the path along which the alternating current flows in the fuel cell is described below.

**[0081]** FIGS. **4**A to **4**D are diagrams schematically showing a path, along which an alternating current superimposed on an output current of the fuel cell **1** flows, in the equivalent circuit model of the fuel cell **1** according to the present embodiment for each frequency band of the alternating current.

**[0082]** FIG. **4**A shows a path of an alternating current of a frequency belonging to a low frequency band, for example, near 0 Hz (hereinafter, also written as a first frequency band). Further, FIG. **4**B shows a path of an alternating current of a frequency belonging to a frequency band slightly higher than the first frequency band by about several Hz (hereinafter, also written as a second frequency band). Furthermore, FIG. **4**C shows a path of an alternating current of a frequency belonging to a frequency band slightly higher than the second frequency band by about several tens of Hz to several KHz (hereinafter, also written as a third frequency band). Further, FIG. **4**D shows a path of an alternating current of a frequency belonging to a highest frequency band of several tens of KHz or higher (hereinafter, also written as a fourth frequency band). Note that the path of the alternating current is shown by a thick line in FIGS. **4**A to **4**D.

**[0083]** First, the value of the alternating current of the frequency belonging to the first frequency band shown in FIG. **4**A moderately varies since the frequency is low, and properties of the alternating current are close to those of a

direct current having a constant current value. Thus, the alternating current having the properties close to those of the direct current does not flow to the electrical double layer capacitance of the anode electrode **112** and the electrical double layer capacitance of the cathode electrode **113** or, even if the alternating current flows, the magnitude thereof is small to a negligible extent. Specifically, as shown in FIG. **4**A, the alternating current substantially flows only to the reaction resistance of the anode electrode **112**, the electrolyte membrane resistance and the reaction resistance of the cathode electrode **113**.

**[0084]** Next, the value of the alternating current of the frequency belonging to the second frequency band shown in FIG. **4**B more largely varies as compared to the alternating current of the frequency belonging to the first frequency band, and properties as the alternating current are intensified. Thus, as shown in FIG. **4**B, the alternating current is thought to start flowing also toward the electrical double layer capacitance of the cathode electrode **113**.

**[0085]** On the other hand, since the reaction resistance value $R_a$ of the anode electrode **112** is known to have a much smaller value than the reaction resistance value $R_c$ of the cathode electrode **113**, the current relatively easily flows toward the reaction resistance of the anode electrode **112**. Thus, it is thought that the alternating current of the frequency in the second frequency band still does not flow toward the electrical double layer capacitance part of the anode electrode **112** or, even if the alternating current flows, the magnitude thereof is small to a negligible extent.

**[0086]** Further, the value of the alternating current of the frequency belonging to the third frequency band shown in FIG. **4**C more largely varies as compared to the alternating current of the frequency belonging to the second frequency band, and properties as the alternating current are further intensified. Thus, the influence of the electrical double layer capacitance of the anode electrode **112** can be no longer ignored and the current is thought to flow also to the electrical double layer capacitance of the anode electrode **112**.

**[0087]** On the other hand, in this third frequency band, an oxidation/reduction reaction in the cathode electrode **13** cannot follow a variation speed of the value of the above alternating current and a state occurs in which this oxidation/reduction reaction does not apparently occur.

**[0088]** Accordingly, the cathode gas substantially does not react in the cathode electrode **113**, wherefore the influence of the reaction resistance of the cathode electrode **113** due to the above oxidation/reduction reaction can be ignored.

**[0089]** Specifically, in the third frequency band, the alternating current does not flow to the reaction resistance of the cathode electrode **113** or, even if the alternating current flows, the magnitude thereof is small to a negligible extent. Thus, the alternating current is thought to substantially flow only to the electrical double layer capacitance component.

**[0090]** It should be noted that performance of the oxidation/reduction reaction to follow a variation of the value of the alternating current is relatively high in the anode electrode **112** and this oxidation/reduction reaction can still follow the variation of the value of the alternating current in the third frequency band. Thus, as shown in FIG. **4**C, the alternating current of the frequency belonging to the third frequency band is thought to still flow through the reaction resistance of the anode electrode **112**.

**[0091]** The value of the alternating current of the frequency belonging to the fourth frequency band shown in FIG. **4**D even more largely varies as compared to the alternating current of the frequency belonging to the third frequency band, wherefore not only the oxidation/reduction reaction in the cathode electrode **113**, but also the oxidation/reduction reaction in the anode electrode **112** can no longer follow the variation of the value of this alternating current.

**[0092]** Accordingly, the reaction substantially does not occur in the anode electrode **112** in addition to in the cathode electrode **113**, and the influence of both the reaction resistance of the cathode electrode **113** and that of the anode electrode **112** can be ignored.

**[0093]** Specifically, in the fourth frequency band, the alternating current does not flow to the reaction resistances of both the cathode electrode **113** and the anode electrode **112** or, even if the alternating current flows, the magnitude thereof is small to a negligible extent. Thus, as shown in FIG. **4**D, the alternating current of the frequency belonging to the fourth frequency band is thought to flow only toward the electrical double layer capacitance of each of the cathode electrode **113** and the anode electrode **112**.

**[0094]** As is understood from the above description, the paths along which the alternating current of the frequency selected from the aforementioned first frequency band, the alternating current of the frequency selected from the aforementioned second frequency band, the alternating current of the frequency selected from the aforementioned third frequency band and the alternating current of the frequency selected from the aforementioned fourth frequency band flow to each element in the simplified equivalent circuit of the fuel cell differ.

**[0095]** Accordingly, the present inventors arrived at individual estimation of various state quantities from impedances based on frequencies belonging to each frequency band with reference to the following equation for impedance obtained on the basis of the simplified equivalent circuit utilizing differences of the paths of the alternating currents corresponding to the frequencies as just described:

[Equation 1]

$$Z = R_m + \frac{R_a(1 - j\omega C_a R_a)}{1 + \omega^2 C_a^2 R_a^2} + \frac{R_c(1 - j\omega C_c R_c)}{1 + \omega^2 C_c^2 R_c^2} \quad (1)$$

(where j denotes an imaginary unit).

**[0096]** For example, the alternating current of the frequency selected from the above fourth frequency band (hereinafter, also written as an "electrolyte membrane response frequency band") flows to the electrolyte membrane resistance, the electrical double layer capacitance of the anode electrode **112** and the electrical double layer capacitance of the cathode electrode **113**. Thus, the impedance based on the frequency selected from this electrolyte membrane response frequency band (hereinafter, also written as an "electrolyte membrane response impedance") includes information of the electrolyte membrane resistance value $R_m$.

**[0097]** It should be noted that this electrolyte membrane response frequency band is a frequency band used in so-called HFR (High Frequency Resistance) measurement. Thus, if $\omega \rightarrow \infty$ is assumed in Equation (1) for impedance, the

impedance Z can be regarded to substantially match the electrolyte membrane resistance value $R_m$.

**[0098]** Further, the alternating current of the frequency selected from the third frequency band (hereinafter, also written as an "anode electrode response frequency band") flows to the electrolyte membrane resistance, the reaction resistance of the anode electrode **112**, the electrical double layer capacitance of the anode electrode **112** and the electrical double layer capacitance of the cathode electrode **113**. Thus, the impedance based on the frequency selected from this anode electrode response frequency band (hereinafter, also written as an "anode electrode response impedance") includes information of at least the reaction resistance value $R_a$ of the anode electrode **112** and the electrical double layer capacitance value $C_a$ of the anode electrode **112**.

**[0099]** Particularly, since the reaction resistance of the cathode electrode **113** can be ignored in the equivalent circuit shown in FIG. **4**C in this case, the following equation for impedance is given.

[Equation 2]

$$Z = R_m + \frac{R_a(1 - j\omega C_a R_a)}{1 + \omega^2 C_a^2 R_a^2} - j\frac{1}{\omega C_c} \quad (2)$$

**[0100]** Further, the alternating current of the frequency selected from the second frequency band flows to the electrolyte membrane resistance, the reaction resistance of the anode electrode **112**, the reaction resistance of the cathode electrode **113** and the electrical double layer capacitance of the cathode electrode **113**. Thus, the impedance based on the frequency selected from this second frequency band includes information of the electrolyte membrane resistance value, the reaction resistance value of the anode electrode **112**, the reaction resistance value $R_c$ of the cathode electrode **113** and the electrical double layer capacitance value $C_c$ of the cathode electrode **113** as state quantities.

**[0101]** Furthermore, the alternating current of the frequency selected from the first frequency band (hereinafter, also written as a "low frequency band"), which is a lowest frequency band, flows to the electrolyte membrane resistance, the reaction resistance of the anode electrode **112** and the reaction resistance of the cathode electrode **113**. Thus, the impedance based on the frequency selected from this low frequency band (hereinafter, also written as an "low frequency response impedance") includes information of at least the reaction resistance value $R_c$ of the cathode electrode **113**.

**[0102]** The estimation of each state quantity using at least two of the above electrolyte membrane response frequency band, anode electrode response frequency band and low frequency band is described in detail in each embodiment below.

**[0103]** It should be noted that it is generally known that there is a relationship of $\omega=2\pi f$ between a "frequency f" and an "angular frequency ω", and there is only a difference multiplied by a dimensionless constant $2\pi$ between these. Thus, the "frequency" and the "angular frequency" are identified with each other and a symbol "ω" is used in expressing the both to facilitate description in each embodiment.

First Embodiment

**[0104]** A first embodiment is described below.

**[0105]** FIG. **5** is a flow chart showing the flow of state quantity estimation according to the present embodiment.

**[0106]** As shown, first in Step **S101**, a frequency $\omega_H$ at one point in the electrolyte membrane response frequency band is selected and an impedance $Z(\omega_H)$ based on the frequency $\omega_H$ is obtained.

**[0107]** Specifically, the controller **6** controls the DC/DC converter **56** such that an alternating-current signal of the frequency $\omega_H$ in the electrolyte membrane response frequency band is superimposed on an output voltage and an output current output from the fuel cell **1** at an impedance measurement timing.

**[0108]** Further, the controller **6** applies a Fourier transform processing on a value V of the output voltage measured by the voltage sensor **52** to obtain a voltage amplitude value $V(\omega_H)$, applies a Fourier transform processing on a value I of the output current measured by the current sensor **51** to obtain a current amplitude value $I(\omega_H)$ and obtains a ratio $V(\omega_H)/I(\omega_H)$ of these as the impedance $Z(\omega_H)$. It should be noted that since a method for measuring the impedance $Z(\omega_H)$ is similar also in the case of measurement for the frequency selected from the anode electrode response frequency band or the low frequency band other than the electrolyte membrane response frequency band, detailed description is omitted hereinafter.

**[0109]** Subsequently, in Step **S102**, the controller **6** estimates the electrolyte membrane resistance value $R_m$ from the obtained impedance $Z(\omega_H)$. Specifically, since the electrolyte membrane response frequency band is a frequency band used in the so-called HFR measurement as described above, the impedance $Z(\omega_H)$ based on the frequency $\omega_H$ selected from this high frequency band or a real component $Z_r(\omega_H)$ thereof substantially matches the electrolyte membrane resistance value $R_m$. Specifically, the value of the impedance $Z(\omega_H)$ or the real component $Z_r(\omega_H)$ thereof is directly estimated as the electrolyte membrane resistance value $R_m$.

**[0110]** In Step **S103**, the controller **6** selects frequencies $\omega_1$, $\omega_2$ at two points in the anode electrode response frequency band and obtains anode electrode response impedances $Z(\omega_1)$, $Z(\omega_2)$ based on these frequencies $\omega_1$, $\omega_2$.

**[0111]** In Step **S104**, the controller **6** estimates the reaction resistance value $R_a$ of the anode electrode **112** and the electrical double layer capacitance value $C_a$ of the anode electrode **112** from the estimated electrolyte membrane resistance value $R_m$ and the obtained two impedances $Z(\omega_1)$, $Z(\omega_2)$.

**[0112]** A mode of this estimation is specifically described. First, in the case of selecting the frequencies $\omega_1$, $\omega_2$ at the two points in the anode electrode response frequency band, the reaction resistance of the cathode electrode **113** can be ignored as described above. Thus, Equation (2) obtained by removing the reaction resistance value $R_c$ of the cathode electrode **113** from Equation (1) for impedance based on the simplified equivalent circuit can be used as an equation for impedance.

**[0113]** Here, the frequencies $\omega_1$, $\omega_2$ at the two points, which are known values, and a combination of the impedances $Z(\omega_1)$ and $Z(\omega_2)$ based on these are substituted into in Equation (2) and real components $Z_r(\omega_1)$ and $Z_r(\omega_2)$ of the impedances $Z(\omega_1)$ and $Z(\omega_2)$ are taken. Considering that the estimated electrolyte membrane resistance value $R_m$ is

known, two equations with $R_a$ and $C_a$ serving as unknowns are obtained. Thus, $R_a$ and $C_a$ can be obtained if the obtained two equations are solved.

**[0114]** An example of a method for obtaining the unknowns $R_a$ and $C_a$ is described. First, if the real component of Equation (2) is taken and changed, the following equation is obtained.

[Equation 3]

$$\frac{1}{Z_r} = \omega^2 C_a^2 R_a + \frac{1}{R_a} - \frac{R_m}{Z_r(Z_r - R_m)} \tag{3}$$

Considering a plane with $\omega^2$ represented on a horizontal axis and $1/Z_r$ represented on a vertical axis, a straight line is represented by Equation (3) on this plane and a gradient $m_r$ thereof is given by the following equation.

**[0115]** [Equation 4]

$$m_r = C_a^2 R_a \tag{4}$$

Here, the frequencies $\omega_1$, $\omega_2$ at the two points are known. Thus, if these frequencies $\omega_1$, $\omega_2$ at the two points and the real components $Z_r(\omega_1)$ and $Z_r(\omega_2)$ of the impedance measurement values corresponding to these frequencies are plotted on the above plane, a straight line connecting these points is determined and the value of the gradient $m_r$ is determined. Specifically, unknowns of Equation (4) are $R_a$ and $C_a$.

**[0116]** Subsequently, an intercept a of the straight line represented by Equation (3) is given by the following equation.

[Equation 5]

$$a = \frac{1}{R_a} - \frac{R_m}{Z_r(Z_r - R_m)} \tag{5}$$

Here, the value of the intercept a is determined by the frequencies $\omega_1$, $\omega_2$ at the points and the real components $Z_{r1}$ and $Z_{r2}$ of the impedance measurement values corresponding to these frequencies similarly to the value of the gradient $m_r$. Since $Z_r$ is equivalent to the real components $Z_{r1}$ and $Z_{r2}$ of the impedance measurement values, only $R_a$ is unknown in Equation (5).

**[0117]** Thus, according to Equation (5), the reaction resistance value $R_a$ of the anode electrode **112** can be obtained as follows.

[Equation 6]

$$R_a = \frac{Z_r(Z_r - R_m)}{Z_r a(Z_r - R_m) + R_m} \tag{6}$$

**[0118]** Further, by substituting $R_a$ determined by Equation (6) into Equation (4), the electrical double layer capacitance value $C_a$ of the anode electrode **112** can be obtained as follows.

[Equation 7]

$$C_a = \sqrt{\frac{m_r}{R_a}} \tag{7}$$

**[0119]** It should be noted that a method for calculating $R_a$ and $C_a$ is not limited to the above calculation method and various suitable calculation methods can be used.

**[0120]** Subsequently, in Step S**105**, the controller **6** selects a frequency $\omega_L$ at one point in the low frequency band and measures an impedance $Z(\omega_L)$ based on this frequency $\omega_L$.

**[0121]** In Step S**106**, the controller **6** estimates the electrical double layer capacitance value $C_c$ of the cathode electrode **113** using the already estimated electrolyte membrane resistance value $R_m$, reaction resistance value $R_a$ of the anode electrode **112** and electrical double layer capacitance value $C_a$ of the anode electrode **112** and the measured impedance $Z(\omega_L)$.

**[0122]** A mode of this estimation is specifically described. An alternating current of the frequency $\omega_L$ in the low frequency band flows to all the circuit elements in the simplified equivalent circuit of the fuel cell **1**, i.e., the reaction resistance and the electrical double layer capacitance of the anode electrode **112**, the electrolyte membrane resistance and the reaction resistance and the electrical double layer capacitance of the cathode electrode **113** as described above. Thus, the low frequency impedance $Z(\omega_L)$ obtained on the basis of the frequency $\omega_L$ includes information of the reaction resistance $R_a$ and the electrical double layer capacitance $C_a$ of the anode electrode **112**, the electrolyte membrane resistance $R_m$ and the reaction resistance $R_c$ and the electrical double layer capacitance $C_c$ of the cathode electrode **113**. Thus, Equation (1) taking into account of all the above circuit elements needs to be used as the equation for impedance.

**[0123]** The frequency $\omega_L$, which is a known value, and the impedance $Z(\omega_L)$ based on this frequency are substituted into Equation (1), and a real component $Z_r(\omega_L)$ and an imaginary component $Z_i(\omega_L)$ are taken. Considering that the estimated electrolyte membrane resistance value $R_m$, reaction resistance value $R_a$ of the anode electrode **112** and electrical double layer capacitance $C_a$ of the anode electrode **112** are known, two equations with $R_c$ and $C_c$ serving as unknowns are obtained. Thus, the unknowns $R_c$ and $C_c$ can be obtained if these two equations are solved.

**[0124]** An example of a method for obtaining the unknowns $R_c$ and $C_c$ is described. First, if the real component of Equation (1) is taken and changed, the following equation is obtained.

[Equation 8]

$$Z_r = R_m + \frac{R_a}{1 + \omega^2 C_a^2 R_a^2} + \frac{R_c}{1 + \omega^2 C_c^2 R_c^2} \tag{8}$$

**[0125]** Further, if the imaginary component of Equation (1) is taken and changed, the following equation is obtained.

[Equation 9]

$$Z_i = \frac{-\omega C_a R_a}{1+\omega^2 C_a^2 R_a^2} + \frac{-\omega C_c R_c}{1+\omega^2 C_c^2 R_c^2} \quad (9)$$

**[0126]** Here, the frequency $\omega_L$, the real component $Zr(\omega_L)$ and the imaginary component $Z_i(\omega_L)$ of the impedance measurement value corresponding to the frequency $\omega_L$ and $R_a$ and $C_a$ are known. If these are substituted into Equations (8) and (9) and Equations are changed, the electrical double layer capacitance value $C_c$ of the cathode electrode **113** is as follows.

[Equation 10]

$$C_c = \frac{1}{\omega R_c}\sqrt{\frac{R_c - A}{A}} \quad (10)$$

**[0127]** In Equation (10), $\omega$ is $\omega_L$ and A is defined as in the following Equation (11).

[Equation 11]

$$A = Z_r - R_m - \frac{R_a}{1+\omega^2 C_a^2 R_a^2} \quad (11)$$

**[0128]** Further, the reaction resistance value $R_c$ of the cathode electrode **113** is obtained as follows.

[Equation 12]

$$R_c = \frac{1-2B^2 \pm \sqrt{1-4B^2}}{2B} A + A \quad (12)$$

**[0129]** A in Equation (12) is defined as in the above Equation (11) and B in Equation (12) is defined as in the following Equation (13).

[Equation 13]

$$B = Z_i + \frac{\omega C_a R_a}{1+\omega^2 C_a^2 R_a^2} \quad (13)$$

**[0130]** As described above, the electrolyte membrane resistance value $R_m$, the reaction resistance value $R_a$ of the anode electrode **112**, the electrical double layer capacitance value $C_a$ of the anode electrode **112**, the reaction resistance value $R_c$ of the cathode electrode **113** and the electrical double layer capacitance value $C_c$ of the cathode electrode **113** are estimated as the state quantities of the fuel cell **1** by Steps **S101** to **S106**.

**[0131]** According to the present embodiment described above, the following effects can be obtained. In the present embodiment, the state detection device is configured by the controller **6**, the current sensor **51**, the voltage sensor **52** and the DC/DC converter **6**. Further, impedance acquisition unit and internal state quantity estimation unit are configured by the controller **6**.

**[0132]** According to the present embodiment, the impedance acquisition unit of the state detection device for the fuel cell **1** for generating power upon receiving the supply of the anode gas and the cathode gas acquires the high frequency impedances $Z(\omega_H)$, $Z(\omega_1)$ and $Z(\omega_2)$ based on the frequencies $\omega_H$, $\omega_1$ and $\omega_2$ selected from the high frequency band (anode electrode response frequency band and electrolyte membrane response frequency band) including a frequency band which shows responsiveness at least to the state quantities $R_a$, $C_a$ of the anode electrode **112** and the low frequency impedance $Z(\omega_L)$ based on the frequency $\omega_L$ selected from the low frequency band including a frequency band which shows responsiveness at least to the state quantities $R_c$, $C_c$ of the cathode electrode (Step **S101**, Step **S103**, Step **S105**).

**[0133]** The internal state quantity estimation unit of the state detection device for the fuel cell **1** estimates each of the state quantities $R_a$, $C_a$ of the anode electrode **112** and the state quantities $R_c$, $C_c$ of the cathode electrode **113** serving as the internal states of the fuel cell **1** by combining the obtained high frequency impedances $Z(\omega_H)$, $Z(\omega_1)$ and $Z(\omega_2)$ and low frequency impedance $Z(\omega_L)$.

**[0134]** According to this, at least each of the state quantities $R_a$, $C_a$ of the anode electrode **112** and the state quantities $R_c$, $C_c$ of the cathode electrode **113** can be individually detected on the basis of the obtained high frequency impedances $Z(\omega_H)$, $Z(\omega_1)$ and $Z(\omega_2)$ and low frequency impedance $Z(\omega_L)$, i.e., impedance information obtained from the different frequency bands, utilizing a following speed difference of the reaction of the anode electrode **112** and the reaction of the cathode electrode **113** in response to a current variation according to the magnitude of the frequency. Thus, highly accurate information of the state quantities $R_a$, $C_a$ of the anode electrode **112** and the state quantities ($R_c$, $C_c$) of the cathode electrode **113** can be obtained, with the result that an operation control of the fuel cell **1** executed utilizing these state quantities can be made more proper.

**[0135]** Further, according to the present embodiment, the internal state quantity estimation unit estimates the internal state quantities $R_m$, $R_a$ and $C_a$ on the basis of the high frequency impedances $Z(\omega_H)$, $Z(\omega_1)$ and $Z(\omega_2)$ and estimates the other internal state quantities $R_c$ and $C_c$ on the basis of the estimated internal state quantities $R_m$, $R_a$ and $C_a$ and the low frequency impedance $Z(\omega_L)$.

**[0136]** In this way, the internal state quantities $R_c$, $C_c$ that cannot be determined only from the low frequency impedance $Z(\omega_L)$ in the low frequency band, which is one frequency band, can be determined on the basis of the internal state quantities $R_m$, $R_a$ and $C_a$ estimated from the high frequency impedances $Z(\omega_H)$, $Z(\omega_1)$ and $Z(\omega_2)$ in the high frequency band, which is another frequency band. Specifically, each of a plurality of types of internal state quantities $R_m$, $R_a$, $C_a$, $R_c$ and $C_c$ can be more reliably distinguished.

**[0137]** It should be noted that the internal state quantity estimation unit may, conversely, estimate a certain internal state quantity on the basis of the low frequency impedance $Z(\omega_L)$ and estimate another internal state quantity on the basis of the estimated internal state quantity and the high frequency impedances $Z(\omega_H)$, $Z(\omega_1)$ and $Z(\omega_2)$.

**[0138]** Further, according to the present embodiment, the above high frequency band (anode electrode response frequency band and electrolyte membrane response frequency band) includes the anode electrode response frequency band, which is a frequency band which shows responsiveness to the state quantities $R_a$, $C_a$ of the anode electrode **112** of the fuel cell **1**, and the electrolyte membrane response frequency band, which is a frequency band higher than the anode electrode response frequency band and which shows responsiveness to the state quantity $R_m$ of the electrolyte membrane of the fuel cell **1**. The impedance acquisition unit acquires both the anode electrode response impedances $Z(\omega_1)$, $Z(\omega_2)$ based on the frequencies selected from the anode electrode response frequency band and the electrolyte membrane response impedance $Z(\omega_H)$ based on the frequency selected from the electrolyte membrane response frequency band as the high frequency impedances $Z(\omega_H)$, $Z(\omega_1)$ and $Z(\omega_2)$ (Step S**101**, Step S**103**).

**[0139]** In this way, each of the state quantity $R_m$ of the electrolyte membrane **111** of the fuel cell **1** and the state quantities $R_a$, $C_a$ of the anode electrode **112** can be estimated on the basis of the electrolyte membrane response impedance $Z(\omega_H)$ and the anode electrode response impedances $Z(\omega_1)$, $Z(\omega_2)$.

**[0140]** Further, according to the present embodiment, the internal state quantity estimation unit estimates the state quantity $R_m$ of the electrolyte membrane **111** on the basis of the electrolyte membrane response impedance $Z(\omega_H)$ (Step S**102**) and estimates the state quantities $R_a$, $C_a$ of the anode electrode **112** on the basis of the estimated electrolyte membrane resistance $R_m$ and the anode electrode response impedances $Z(\omega_1)$, $Z(\omega_2)$ (Step S**104**).

**[0141]** In this way, the state quantities $R_a$, $C_a$ of the anode electrode **112** can be estimated in clearer distinction from the other state quantities on the basis of the estimated state quantity $R_m$ of the electrolyte membrane **111** and the anode electrode response impedances $Z(\omega_1)$, $Z(\omega_2)$.

**[0142]** Particularly, in the present embodiment, the state quantities $R_a$, $C_a$ of the anode electrode **112** include the reaction resistance value $R_a$ and the electrical double layer capacitance value $C_a$ of the anode electrode **112**, and the state quantities $R_c$, $C_c$ of the cathode electrode **113** include the reaction resistance value $R_c$ and the electrical double layer capacitance value $C_c$ of the cathode electrode **113**. The internal state quantity estimation unit estimates the reaction resistance value $R_a$ of the anode electrode **112** and the electrical double layer capacitance value $C_a$ of the anode electrode **112** on the basis of the anode electrode response impedance $Z(\omega_1)$, $Z(\omega_2)$ (Step S**104**). Further, the internal state quantity estimation unit estimates the reaction resistance value $R_c$ of the cathode electrode **113** on the basis of the estimated state quantity $R_m$ of the electrolyte membrane **111**, reaction resistance value $R_a$ of the anode electrode **112**, electrical double layer capacitance value $C_a$ of the anode electrode **112** and the low frequency impedance $Z(\omega_L)$ (Step S**106**).

**[0143]** According to this, the reaction resistance value $R_a$ and the electrical double layer capacitance value $C_a$ of the anode electrode **112** estimated on the basis of the anode electrode response impedances ($Z(\omega_1)$, $Z(\omega_2)$) and the state quantity $R_m$ of the electrolyte membrane **111** estimated on the basis of the electrolyte membrane response impedance $Z(\omega_H)$ can be applied to the low frequency impedance $Z(\omega_L)$ in the low frequency band including all pieces of information other than the reaction resistance value $R_c$ of the cathode electrode **113**.

**[0144]** Accordingly, the targeted state quantity $R_c$ can be suitably distinguished and estimated from the low frequency impedance $Z(\omega_L)$ in the low frequency band including information other than the targeted state quantity $R_c$.

## Second Embodiment

**[0145]** A second embodiment is described below. It should be noted that elements similar to those of the already described first embodiment are denoted by the same reference signs.

**[0146]** FIG. **6** is a flow chart showing the flow of state quantity estimation according to the second embodiment. Since Steps S**101** to S**104** in FIG. **6** are similar to Steps S**101** to S**104** in FIG. **5**, no detailed description is given. In the second embodiment, a gradient of a straight part of a characteristic curve in an I-V characteristic curve diagram (I-V characteristic diagram) of a fuel cell **1** set in advance is regarded and acquired as a low frequency impedance instead of measuring a low frequency impedance at a frequency in a low frequency band.

**[0147]** As shown, after Steps S**101** to S**104**, i.e., estimation values of the reaction resistance value $R_a$ and the electrical double layer capacitance value $C_a$ of the anode electrode **112** are acquired, the gradient $\Delta V/\Delta I$ of the straight part of the characteristic curve in the I-V characteristic diagram of the fuel cell **1** is regarded and acquired as the low frequency impedance $Z(\omega_L)$ in Step S**205**.

**[0148]** FIG. **7** shows I-V characteristic curves of the fuel cell **1** respectively in steady time and in unsteady time. It should be noted that these I-V characteristic curves of the fuel cell **1** are determined in advance on the basis of an experiment or the like. A characteristic curve Cv**1** shows an I-V characteristic in steady time and a characteristic curve Cv**2** shows an I-V characteristic in unsteady time. Here, the I-V characteristic in steady time means an output characteristic of the fuel cell **1** during stable travel not in a sudden accelerating state such as during vehicle startup or during vehicle stop.

**[0149]** Particularly, as understood from FIG. **7**, a variation of the gradient $\Delta V/\Delta I$ is small, has a substantially constant value and is linear in a steady region P of the characteristic curve Cv**1** in steady time. Thus, in the steady region P, the gradient $\Delta V/\Delta I$ can be regarded as a constant value regardless of an output current I.

**[0150]** As just described, the steady region P where the value of $\Delta V/\Delta I$ is constant is a section of a horizontal axis (output current I) in which the value of $\Delta V/\Delta I$ of the characteristic curve Cv**1** in steady time is not larger than a predetermined value.

**[0151]** In the present embodiment, the controller **6** stores the value of $\Delta V/\Delta I$ in this steady region P in an unillustrated memory or the like in advance, reads the value of $\Delta V/\Delta I$ from this memory at an acquisition timing of the low frequency impedance $Z(\omega_L)$ and regards this value as the low frequency impedance $Z(\omega_L)$. The low frequency impedance $Z(\omega_L)$ obtained in this way matches well an actual value.

**[0152]** In Step S**206**, the reaction resistance value $R_c$ of the cathode electrode **113** is estimated using the value of $\Delta V/\Delta I$ acquired as the low frequency impedance $Z(\omega_L)$.

**[0153]** This is specifically described. If ω is assumed to be a low frequency (ω→0) in Equation (1) described above, the following equation is thought to hold.

[Equation 14]

$$\lim_{\omega \to 0} Z = R_m + R_a + R_c \tag{14}$$

Thus, if the impedance Z is substituted by ΔV/ΔI in Equation (14), the following equation is obtained.

[Equation 15]

$$R_c = \frac{\Delta V}{\Delta I} - R_m - R_a \tag{15}$$

**[0154]** In this way, the reaction resistance value $R_c$ of the cathode electrode **113** can be calculated by substituting the electrolyte membrane resistance value $R_m$ estimated in the process of Steps S**101** to S**104** and the reaction resistance value $R_a$ of the anode electrode **112** into Equation (15).

**[0155]** According to the state detection device for the fuel cell **1** according to the present embodiment described above, the controller **6** serving as the impedance acquisition unit acquires the gradient ΔV/ΔI of the I-V characteristic curve of the fuel cell **1** as the low frequency impedance $Z(\omega_1)$. Specifically, the low frequency impedance $Z(\omega_1)$ can be acquired without being directly measured.

**[0156]** It should be noted that the low frequency impedances $Z(\omega_1)$ may be acquired by both methods for acquiring the low frequency impedance $Z(\omega_1)$ as the value of the gradient ΔV/ΔI of the I-V characteristic curve and acquiring the low frequency impedance $Z(\omega_1)$ by measurement and the highly accurate low frequency impedance $Z(\omega_1)$ acquired such as by comparing/correcting the low frequency impedances $Z(\omega_1)$ obtained by these two methods may be used for the estimation of the reaction resistance value $R_c$ of the cathode electrode **113**.

**[0157]** Further, in the present embodiment, the controller **6** serving as the impedance acquisition unit acquires the gradient ΔV/ΔI as the low frequency impedance $Z(\omega_1)$ in the steady region P where the variation of the value of the gradient in the I-V characteristic curve Cv**1** of the fuel cell **1** is not larger than the predetermined value.

**[0158]** As just described, in the steady region P where the variation of the gradient ΔV/ΔI is relatively small, there is no problem in regarding the value of the gradient ΔV/ΔI as constant regardless of a measurement value of the output current I. Thus, it is not necessary to calculate the value of the gradient ΔV/ΔI for each of the measurement values of the output voltage V and the output current I and the amount of calculation can be reduced.

## Third Embodiment

**[0159]** A third embodiment is described below. It should be noted that elements similar to those of the already described embodiments are denoted by the same reference signs.

**[0160]** FIG. **8** is a flow chart showing the flow of state quantity estimation according to the present embodiment. As shown, the estimation of the electrolyte membrane resistance value $R_m$ using the frequency in the electrolyte membrane response frequency band equivalent to Steps S**101** and S**102** shown in FIG. **5** is omitted.

**[0161]** Particularly, in the present embodiment, the reaction resistance value $R_a$ of the anode electrode **112**, the electrical double layer capacitance value $C_a$ of the anode electrode **112**, the electrical double layer capacitance value $C_c$ of the cathode electrode **113** and the electrolyte membrane resistance value $R_m$ serving as state quantities are estimated, using anode electrode response impedances $Z(\omega_1)$, $Z(\omega_2)$ acquired at two frequencies $\omega_1$, $\omega_2$ in the anode electrode response frequency band in specific Step S**304** (Step S**304**).

**[0162]** A mode of the state quantity estimation in Step S**304** is described below.

**[0163]** Also in the present embodiment, calculation is performed on the basis of Equation (2) for impedance described above. A step of obtaining Equation (3) by taking a real component of Equation (2) and obtaining Equation (4) on the basis of Equation (3) is as in the case of estimating the reaction resistance value $R_a$ of the anode electrode **112** and the electrical double layer capacitance value $C_a$ of the anode electrode **112** according to the first embodiment.

**[0164]** If Equation (4) is changed, the following equation is obtained.

[Equation 16]

$$R_a = \frac{m_r}{C_a^2} \tag{16}$$

It should be noted that $m_r$ is a gradient of a straight line connecting two impedances $Z(\omega_1)$ and $Z(\omega_2)$ and a known value as described above.

**[0165]** On the other hand, if an imaginary component of Equation (2) is taken, the following equation is obtained.

[Equation 17]

$$Z_i = -\frac{\omega C_a R_a^2}{1 + \omega^2 C_a^2 R_a^2} - \frac{1}{\omega C_c} \tag{17}$$

**[0166]** Here, if $R_a$ of Equation (16) is substituted into the above Equation (17) and both sides are multiplied by ω, the following equation is obtained.

[Equation 18]

$$\omega Z_i = -\frac{\omega^2 m_r^2}{C_a^3 + \omega^2 m_r^2 C_a} - \frac{1}{C_c} \tag{18}$$

**[0167]** If the above known frequencies $\omega_1$ and $\omega_2$ and imaginary components $Z_{i1}$ and $Z_{i2}$ of impedance measurement values corresponding to these frequencies are respectively substituted into Equation (18) to obtain two equations and the electrical double layer capacitance $C_c$ of the cathode is erased by taking a difference between these two equations, the following quartic equation for the unknown electrical double layer capacitance $C_a$ of the anode is obtained.

[Equation 19]

$$C_a^4 + (\omega_1^2 + \omega_2^2)m_r^2 C_a^2 + \frac{\omega_1^2 - \omega_2^2}{\omega_1 Z_{i1} - \omega_2 Z_{i2}} m_r^2 C_a + \omega_1^2 \omega_2^2 m_r^4 = 0 \quad (19)$$

**[0168]** When the quartic equation of Equation (19) is solved and it is considered that $C_a$ cannot be an imaginary value, the following two solutions are obtained as candidates for the electrical double layer capacitance $C_a$ of the anode.

[Equation 20]

$$C_{a1} = \frac{\sqrt{t_1} + \sqrt{-t_1 - 2m_r^2\left(\omega_1^2 + \omega_2^2 + \frac{\omega_1^2 - \omega_2^2}{\sqrt{t_1}\,(\omega_1 Z_{i1} - \omega_2 Z_{i2})}\right)}}{2} \quad (20)$$

[Equation 21]

$$C_{a2} = \frac{\sqrt{t_1} - \sqrt{-t_1 - 2m_r^2\left(\omega_1^2 + \omega_2^2 + \frac{\omega_1^2 - \omega_2^2}{\sqrt{t_1}\,(\omega_1 Z_{i1} - \omega_2 Z_{i2})}\right)}}{2} \quad (21)$$

It should be noted that the quartic equation of Equation (19) can be solved by various methods known to a person skilled in the art.

**[0169]** Here, $t_1$ is a constant defined as follows.

[Equation 22]

$$t_1 = \sqrt[3]{-\frac{27A_0 + 2A_2^3 - 9A_2A_1}{54} + \sqrt{\left(\frac{27A_0 + 2A_2^3 - 9A_2A_1}{54}\right)^2 + \left(\frac{3A_1 - A_2^2}{9}\right)^3}} + \sqrt[3]{-\frac{27A_0 + 2A_2^3 - 9A_2A_1}{54} - \sqrt{\left(\frac{27A_0 + 2A_2^3 - 9A_2A_1}{54}\right)^2 + \left(\frac{3A_1 - A_2^2}{9}\right)^3}} \quad (22)$$

**[0170]** Although the embodiments of the present invention have been described above, the above embodiments are merely an illustration of some application examples of the present invention and not intended to limit the technical scope of the present invention to the specific configurations of the above embodiments.

**[0171]** Further, $A_2$, $A_1$ and $A_0$ in Equation are respectively as follows.

[Equation 23]

$$A_2 = 2(\omega_1^2 + \omega_2^2)m_r^2$$
$$A_1 = (\omega_1^2 + \omega_2^2)^2 m_r^4 - 4\omega_1^2\omega_2^2 m_r^4 \quad (23)$$
$$A_0 = -\left(\frac{\omega_1^2 - \omega_2^2}{\omega_1 Z_{i1} - \omega_2 Z_{i2}}\right)^2 m_r^4$$

**[0172]** Further, by substituting each of $C_{a1}$ and $C_{a2}$ into the above Equation (16), $R_{a1}$ and $R_{a2}$ are determined as candidates for the estimation value of the reaction resistance in correspondence with $C_{a1}$ and $C_{a2}$. The candidates $R_{a1}$ and $R_{a2}$ for the estimation value are as follows.

[Equation 24]

$$R_{a1} = \frac{4m_r}{\left\{\sqrt{t_1} + \sqrt{-t_1 - 2m_r^2\left(\omega_1^2 + \omega_2^2 + \frac{\omega_1^2 - \omega_2^2}{\sqrt{t_1}\,(\omega_1 Z_{i1} - \omega_2 Z_{i2})}\right)}\right\}^2} \quad (24)$$

[Equation 25]

$$R_{a2} = \frac{4m_r}{\left\{\sqrt{t_1} - \sqrt{-t_1 - 2m_r^2\left(\omega_1^2 + \omega_2^2 + \frac{\omega_1^2 - \omega_2^2}{\sqrt{t_1}\,(\omega_1 Z_{i1} - \omega_2 Z_{i2})}\right)}\right\}^2} \quad (25)$$

**[0173]** Here, it is necessary to determine a true estimation value conforming to an actual characteristic from the aforementioned candidates $C_{a1}$ and $C_{a2}$ for the electrical double layer capacitance value of the anode electrode **112** and candidates $R_{a1}$ and $R_{a2}$ for the reaction resistance value. An example of that method is described.

**[0174]** In the present embodiment, the determination of this true estimation value is judged not only from the values of $C_{a1}$, $R_{a1}$, $C_{a2}$ and $R_{a2}$, but also by the following equation for the electrical double layer capacitance value $C_c$ of the cathode electrode **113** obtained by changing the equation for the impedance imaginary component in the above Equation (17).

[Equation 26]

$$C_c = -\frac{1 + \omega^2 C_a^2 R_a^2}{\omega^2 C_a R_a^2 + \omega Z_i (1 + \omega^2 C_a^2 R_a^2)} \quad (26)$$

**[0175]** FIG. **9** shows frequency responses of the candidates $C_{c1}$ and $C_{c2}$ for the electrical double layer capacitance value of the cathode electrode **113**. It should be noted that this graph is based on data of the candidates $C_{a1}$ and $C_{a2}$ for the electrical double layer capacitance value obtained by continuously changing the frequencies $\omega_1$ and $\omega_2$ calculated by an experiment or the like in advance in a range of the anode electrode response frequency band.

**[0176]** It should be noted that a line of $C_{c1}$ is represented by a broken line and a line of $C_{c2}$ is represented by a solid line. Further, a frequency $\omega_d$ is a frequency at which ($C_{a1}$,

$R_{a1}$) =($C_{a2}$, $R_{a2}$) for sets ($C_{a1}$, $R_{a1}$), ($C_{a2}$, $R_{a2}$) of the candidates for the reaction resistance value and the electrical double layer capacitance value of the anode electrode **112**. Specifically, the inside of the radical sign in the above Equations (20), (21), (24) and (25) expressing $C_{a1}$ and $R_{a1}$ $C_{a2}$ and $R_{a2}$ is 0.

**[0177]** As shown, in a region where the frequency $\omega<\omega_d$, the estimation value candidate $C_{c2}$ for the electrical double layer capacitance value is basically 0 or smaller and the value of $C_{c2}$ is extremely sensitive to a change of the frequency immediately before $\omega_d$. Thus, in the region where the frequency $\omega<\omega_d$, $C_{c1}$ is a true estimation value which should be actually employed.

**[0178]** Accordingly, also for the electrical double layer capacitance value and the reaction resistance value of the cathode electrode **113**, $C_{a1}$ and $R_{a1}$ corresponding to $C_{c1}$ are respectively employed in the region where the frequency $\omega<\omega_d$.

**[0179]** On the other hand, in a region where $\omega>\omega_d$, it is difficult to judge which of $C_{c1}$ and $C_{c2}$ should be employed only by looking at changes of the candidates ($C_{c1}$, $C_{c2}$) for the electrical double layer capacitance value of the cathode electrode **113**. Accordingly, this judgment is made by directly studying the sets ($C_{a1}$, $R_{a1}$), ($C_{a2}$, $R_{a2}$) of the candidates for the reaction resistance value and the electrical double layer capacitance value of the anode electrode **112**.

**[0180]** FIG. **10**A shows frequency responses of the candidates $C_{a1}$, $C_{a2}$ for the electrical double layer capacitance value of the anode electrode **112**. Further, FIG. **10**B shows frequency responses of the candidates $R_{a1}$, $R_{a2}$ for the reaction resistance value of the anode electrode **112**. It should be noted that these graphs are also based on data of the sets ($C_{a1}$, $R_{a1}$), ($C_{a2}$, $R_{a2}$) of the candidates obtained by continuously changing the frequencies $\omega_1$ and $\omega_2$ calculated by an experiment or the like in advance in the range of the anode electrode response frequency band.

**[0181]** With reference to FIG. **10**A, in a region where the frequency $\omega>\omega_d$, the candidate $C_{a1}$ for the electrical double layer capacitance value of the anode electrode **112** is extremely sensitive to the frequency. Thus, in the region where $\omega>\omega_d$, $C_{a2}$ is a value which should be actually employed as a true estimation value of the electrical double layer capacitance value of the anode electrode **112**. Therefore, in the region where the frequency $\omega>\omega_d$, $C_{a2}$ and $R_{a2}$ corresponding thereto should be respectively employed.

**[0182]** It should be noted that, as understood with reference to FIG. **10**B, the candidate $R_{a2}$ for the reaction resistance value is extremely sensitive to a frequency change in a region of $\omega<\omega_d$ where the frequency $\omega_d$ is smaller. Thus, the candidate $R_{a1}$ for the reaction resistance value is judged to be a true estimation value which should be actually employed. Thus, in the region where the frequency $\omega<\omega_d$, $C_{a1}$ corresponding to $R_{a1}$ and $R_{a1}$ should be respectively employed. This point is found to match considerations based on the frequency response of the electrical double layer capacitance value of the cathode electrode **113**.

**[0183]** Further, when the frequency $\omega=\omega_d$, ($C_{a1}$, $R_{a1}$)= ($C_{a2}$, $R_{a2}$). Thus, it does not matter which of these sets of the candidates is employed as the set of the true candidates.

**[0184]** Based on the above considerations, it is found that values to be determined from the sets ($C_{a1}$, $R_{a1}$) and ($C_{a2}$, $R_{a2}$) of the candidates change according to the frequency in determining the true estimation values.

**[0185]** Specifically, the appropriate one of the sets ($C_{a1}$, $R_{a1}$) and ($C_{a2}$, $R_{a2}$) of the candidates is determined according to the frequencies $\omega_1$, $\omega_2$ at two points in the anode electrode response frequency band and the magnitude of the frequency $\omega_d$. Further, if the determined estimation values of the electrical double layer capacitance value $C_a$ and reaction resistance value $R_a$ of the anode electrode **112** are substituted into Equation (3), the electrolyte membrane resistance value $R_m$ is obtained since the frequency $\omega$ and the real component $Z_r$ of the impedance measurement value are known.

**[0186]** Subsequent Steps **S105** and **S106** are performed as in the first embodiment to also estimate the reaction resistance value $R_c$ of the cathode electrode **113**, using the estimation values of the electrical double layer capacitance value $C_a$ and reaction resistance value $R_a$ of the anode electrode **112** and the electrolyte membrane resistance value $R_m$ obtained in this way.

**[0187]** According to the state detection for the fuel cell **1** according to the present embodiment described above, only the anode electrode response impedances $Z(\omega_1)$ and $Z(\omega_2)$ are acquired as the high frequency impedances and the state quantities $C_a$ and $R_a$ of the anode electrode **112** are estimated on the basis of the anode electrode response impedances $Z(\omega_1)$ and $Z(\omega_2)$ by the controller **6** serving as the impedance acquisition unit and the internal state quantity estimation unit.

**[0188]** In this way, the state quantities $C_a$ and $R_a$ of the anode electrode **112** can be estimated while reducing a load to the controller **6** by omitting the estimation of the electrolyte membrane resistance value $R_m$ on the basis of the measurement of the electrolyte membrane response impedance and, finally, the reaction resistance value $R_c$, which is the state quantity of the cathode electrode **113**, can be estimated.

## Fourth Embodiment

**[0189]** A fourth embodiment is described. It should be noted that elements similar to those of the already described embodiments are denoted by the same reference signs.

**[0190]** FIG. **11** is a flow chart showing the flow of state quantity estimation according to the present embodiment. As shown, in the present embodiment, the anode electrode response impedances $Z(\omega_1)$ and $Z(\omega_2)$ are obtained in Step **S103** and the estimation values of the reaction resistance value $R_a$ and electrical double layer capacitance value $C_a$ of the anode electrode **112**, the electrical double layer capacitance value $C_c$ of the cathode electrode **113** and the electrolyte membrane resistance value $R_m$ are obtained in Step **S304** as in the third embodiment.

**[0191]** Thus, as in the second embodiment, the low frequency impedance $\Delta V/\Delta I$ is acquired on the basis of the I-V characteristic of the fuel cell **1** in Step **S205** and the reaction resistance value $R_c$ of the cathode electrode **113** is estimated from the estimation values of the low frequency impedance $\Delta V/\Delta I$ and the electrolyte membrane resistance value $R_m$ in Step **S206**.

**[0192]** Accordingly, according to the state detection of the fuel cell **1** according to the present embodiment, the low frequency impedance $Z(\omega_L)$ can be estimated without being directly measured and the estimation of the electrolyte membrane resistance value $R_m$ on the basis of the measure-

ment of the electrolyte membrane response impedance can be omitted. Thus, a load to the controller **6** can be further reduced.

## Fifth Embodiment

**[0193]** A fifth embodiment is described. It should be noted that elements similar to those of the already described embodiments are denoted by the same reference signs.

**[0194]** In the present embodiment, measurement values of actual output voltage V and output current I are used to calculate the value of ΔV/ΔI instead of a mode of storing the value of ΔV/ΔI in the steady region P of the characteristic curve Cv**1** in steady time of FIG. **7** in Step S**205** according to the second and fourth embodiments.

**[0195]** FIG. **12** shows an I-V characteristic curve of the fuel cell **1** in steady time. Particularly, in the present embodiment, the gradient ΔV/ΔI is calculated by calculating $-(V_1-V_2)/(I_1-I_2)$ for output currents $I_1$, $I_2$ measured by the current sensor **51** at predetermined measurement timings and output voltages $V_1$, $V_2$ measured by the voltage sensor **52** at the same predetermined measurement timings.

**[0196]** Specifically, the gradient ΔV/ΔI regarded as the low frequency impedance is determined according to the measurement values of the output currents and the output voltages.

**[0197]** In the present embodiment, the gradient ΔV/ΔI in the I-V characteristic curve of the fuel cell **1** is calculated on the basis of two sets ($I_1$, $V_1$), ($I_2$, $V_2$) of the measurement values of the current and the voltage as just described. In this way, the value of ΔV/ΔI more accurately reflecting an actual characteristic than in the case of using the gradient ΔV/ΔI regarded and determined as a constant value in the steady region P can be obtained. As a result, the accuracy of the estimation value of the reaction resistance value $R_c$ of the cathode electrode **113** calculated assuming this value of ΔV/ΔI as the low frequency impedance is also improved.

## Sixth Embodiment

**[0198]** A sixth embodiment is described. It should be noted that elements similar to those of the already described embodiments are denoted by the same reference signs.

**[0199]** In the present embodiment, in order to obtain the gradient ΔV/ΔI in the I-V characteristic curve, the gradient ΔV/ΔI in the I-V characteristic curve is calculated using one set ($I_3$, $V_3$) of measurement values of the output current and the output voltage and one set ($I_{set}$, $V_{set}$) set beforehand instead of measuring two sets ($I_1$, $V_1$), ($I_2$, $V_2$) of the measurement values of the output current and the output voltage as in the fifth embodiment.

**[0200]** FIG. **13** is a graph showing an example of a method for setting one set of current and voltage for the calculation of the gradient ΔV/ΔI in the I-V characteristic curve. It should be noted that, in this graph, the characteristic curve Cv**1** in steady time is shown by a broken line to clarify the drawing. As shown, a point shown by a black square of FIG. **13** is equivalent to ($I_{set}$, $V_{set}$) described above in the present embodiment. Particularly, $I_{set}=0$.

**[0201]** Accordingly, the value of the gradient ΔV/ΔI is calculated by calculating $-(V_{set}-V_3)/(I_{set}-I_3)$ on the basis of the above measurement values ($I_3$, $V_3$) and the preset values ($I_{set}$, $V_{set}$).

**[0202]** As described above, according to the present embodiment, the value of the gradient ΔV/ΔI in the I-V characteristic curve is calculated on the basis of one set ($I_3$, $V_3$) of the measurement values of the current and the voltage and one set ($I_{set}$, $V_{set}$) of the values of the current and the voltage set beforehand.

**[0203]** Accordingly, in calculating the gradient ΔV/ΔI in the I-V characteristic curve of the fuel cell **1**, it is possible to ensure calculation accuracy of a specified level or higher by using the measurement values ($I_3$, $V_3$) at one point while suppressing the amount of calculation using ($I_{set}$, $V_{set}$) set beforehand at another point out of two points on the I-V characteristic curve used to calculate the value of the gradient.

## Seventh Embodiment

**[0204]** A seventh embodiment is described. It should be noted that elements similar to those of the already described embodiments are denoted by the same reference signs.

**[0205]** In the present embodiment, in the measurement of the impedance of the fuel cell **1** performed in the first embodiment and the like, an excitation current application method in which a current I is supplied from a predetermined current source for measurement to the fuel cell **1** and an impedance Z=V/I is calculated on the basis of this supplied current I and an output voltage V is employed instead of the configuration for measuring the output current I and the output voltage V superimposed with the alternating-current signal.

**[0206]** FIG. **14** is a block diagram schematically showing a main part relating to an impedance measurement in a fuel cell system **100** according to the present embodiment.

**[0207]** As shown, the fuel cell system **100** according to the present embodiment includes an applied alternating current adjustment unit **200** configured to apply an alternating current to a fuel cell **1** while adjusting the alternating current.

**[0208]** The applied alternating current adjustment unit **200** is connected to an intermediate terminal **1**C besides a positive electrode terminal (cathode electrode side terminal) **1**B and a negative electrode terminal (anode electrode side terminal) **1**A of a fuel cell **1** configured as a stack. It should be noted that a part connected to the intermediate terminal **1**C is grounded as shown.

**[0209]** The applied alternating current adjustment unit **200** includes a positive electrode side voltage measurement sensor **210** configured to measure a positive electrode side alternating-current potential difference V**1** of the positive electrode terminal **1**B with respect to the intermediate terminal **1**C and a negative electrode side voltage measurement sensor **212** configured to measure a negative electrode side alternating-current potential difference V**2** of the negative electrode terminal **1**A with respect to the intermediate terminal **1**C.

**[0210]** Further, the applied alternating current adjustment unit **200** includes a positive electrode side alternating-current power supply unit **214** configured to apply an alternating current I**1** to a circuit composed of the positive electrode terminal **1**B and the intermediate terminal **1**C, a negative electrode side alternating-current power supply unit **216** configured to apply an alternating current **12** to a circuit composed of the negative electrode terminal **1**A and the intermediate terminal **1**C, a controller **218** configured to adjust amplitudes and phases of these alternating currents I**1** and I**2**, and a calculation unit 220 configured to calculate an

impedance Z of the fuel cell **1** on the basis of the electrode side alternating-current potential differences V**1**, V**2** and the alternating currents I**1**, I**2**.

**[0211]** In the present embodiment, the controller **218** adjusts the amplitudes and phases of the alternating currents I**1** and I**2** such that the positive electrode side alternating-current potential difference V**1** and the negative electrode side alternating-current potential difference V**2** become equal. It should be noted that this controller **218** may be configured by the controller **6** shown in FIG. **3**.

**[0212]** Further, the calculation unit **220** includes hardware such as an unillustrated AD converter and a microcomputer chip and software configuration such as a program for calculating the impedance, calculates an impedance Z**1** from the intermediate terminal **1**C to the positive electrode terminal **1**B by dividing the positive electrode side alternating-current potential difference V**1** by the alternating current I**1** and calculates an impedance Z**2** from the intermediate terminal **1**C to the negative electrode terminal **1**A by dividing the negative electrode side alternating-current potential difference V**2** by the alternating current I**2**. Furthermore, the calculation unit **220** calculates the total impedance Z of the fuel cell **1** by taking the sum of the impedances Z**1** and Z**2**.

**[0213]** According to a state detection device for fuel cell according to the above embodiment, the following effects can be obtained.

**[0214]** The state detection device for fuel cell according to the present embodiment includes the alternating-current power supply units **214**, **216** connected to the fuel cell **1** and configured to output the alternating currents I**1**, I**2** to the fuel cell **1**, the controller **218** serving as an alternating current adjustment unit configured to adjust the alternating currents I**1**, I**2** on the basis of the positive electrode side alternating-current potential difference V**1**, which is a potential difference obtained by subtracting the potential of the intermediate terminal **1**C from the potential of the positive electrode terminal **1**B of the fuel cell **1**, and the negative electrode side alternating-current potential difference V**2**, which is a potential difference obtained by subtracting the potential of the intermediate terminal **1**C from the potential of the negative electrode terminal **1**A of the fuel cell **1**, and the impedance calculation unit **220** configured to calculate the impedance Z of the fuel cell **1** on the basis of the adjusted alternating currents I**1**, I**2** and the positive electrodes alternating-current potential difference V**1** and the negative electrode side alternating-current potential difference V**2**.

**[0215]** The controller **218** adjusts the amplitudes and phases of the alternating current I**1** applied by the positive electrode side alternating-current power supply unit **214** and the alternating current I**2** applied by the negative electrode side alternating-current power supply unit **216** such that the positive electrode side alternating-current potential difference V**1** on the positive electrode side of the fuel cell **1** and the negative electrode side alternating-current potential difference V**2** on the negative electrode side substantially match. Since the amplitude of the positive electrode side alternating-current potential difference V**1** and that of the negative electrode side alternating-current potential difference V**2** become equal in this way, the positive electrode terminal **1**B and the negative electrode terminal **1**A are substantially at an equal potential. Thus, the alternating currents I**1**, I**2** for the impedance measurement are prevented from flowing to a load **53**, wherefore the influence of the fuel cell **1** on power generation is prevented.

**[0216]** Further, in the case of carrying out the above impedance measurement when the fuel cell **1** is in a power generation state, an alternating-current potential for measurement is superimposed on a voltage generated by this power generation. Thus, the values of the positive electrode side alternating-current potential difference V**1** and the negative electrode side alternating-current potential difference V**2** themselves become larger. However, since the phases and amplitudes of the positive electrode side alternating-current potential difference V**1** and the negative electrode side alternating-current potential difference V**2** themselves do not change, a highly accurate impedance measurement can be carried out as in the case where the fuel cell **1** is not in the power generation state.

**[0217]** Although the embodiments of the present invention have been described above, the above embodiments are merely an illustration of some application examples of the present invention and not intended to limit the technical scope of the present invention to the specific configurations of the above embodiments. For example, the steps of acquiring the anode electrode response impedance, the electrolyte membrane response impedance and the low frequency impedance (Steps, S**101**, S**103** and S**105**) and the like in each embodiment can be arbitrarily changed without being limited to the sequence of the steps described in each embodiment.

**[0218]** For example, each state quantity may be estimated after all the steps of acquiring the anode electrode response impedance, the electrolyte membrane response impedance and the low frequency impedance are performed.

**[0219]** Further, the modes of estimating a plurality of internal state quantities in the fuel cell **1** are not limited to the modes described in each of the above embodiments.

**[0220]** For example, instead of the mode of selecting one frequency $\omega_L$ from the low frequency band in Step S**105** in the first or third embodiment, two frequencies $\omega_{L1}$, $\omega_{L2}$ may be selected in the low frequency band and low frequency impedances $Z(\omega_{L1})$ and $Z(\omega_{L2})$ may be obtained. In this way, not only the estimation value of the reaction resistance $R_c$ of the cathode electrode **113**, but also that of the electrical double layer capacitance $C_c$ of the cathode electrode **113** can be finally obtained.

**[0221]** Further, the mode of the simplified equivalent circuit of the fuel cell **1** is also not limited to that used in each of the above embodiments. For example, an equivalent circuit including other elements such as a diffusion resistance, an electron transport resistance and an ionomer resistance besides the circuit elements such as the reaction resistance and the electrical double layer capacitance of each electrode described in each of the above embodiments may be set, and a diffusion resistance value, an electron transport resistance value, an ionomer resistance value and the like serving as internal state quantities based on these other elements may be estimated.

**1.-12.** (canceled)

**13.** A state detection method for a fuel cell for generating power upon receiving a supply of anode gas and cathode gas, comprising:

a step of acquiring a high frequency impedance based on a frequency selected from a high frequency band and a low frequency impedance based on a frequency selected from a low frequency band, the high frequency band including a frequency band which shows responsiveness at least to a state quantity of an anode elec-

trode, the low frequency band including a frequency band which shows responsiveness at least to a state quantity of a cathode electrode; and

a step of estimating each of the state quantity of the anode electrode and the state quantity of the cathode electrode serving as internal states of the fuel cell by combining the acquired high frequency impedance and low frequency impedance.

**14**. A state detection device for a fuel cell for generating power upon receiving a supply of anode gas and cathode gas, comprising:

an impedance acquisition unit configured to acquire a high frequency impedance based on a frequency selected from a high frequency band and a low frequency impedance based on a frequency selected from a low frequency band, the high frequency band including a frequency band which shows responsiveness at least to a state quantity of an anode electrode, the low frequency band including a frequency band which shows responsiveness at least to a state quantity of a cathode electrode; and

an internal state quantity estimation unit configured to estimate each of the state quantity of the anode electrode and the state quantity of the cathode electrode by combining the acquired high frequency impedance and low frequency impedance, the state quantity of the anode electrode and the state quantity of the cathode electrode serving as internal states of the fuel cell.

**15**. The state detection device for the fuel cell according to claim **14**, wherein the internal state quantity estimation unit:

estimates a certain internal state quantity on the basis of the high frequency impedance and estimates another internal state quantity on the basis of the estimated internal state quantity and the low frequency impedance; or

estimates a certain internal state quantity on the basis of the low frequency impedance and estimates another internal state quantity on the basis of the estimated internal state quantity and the high frequency impedance.

**16**. The state detection device for the fuel cell according to claim **14**, wherein

the high frequency band includes an anode electrode response frequency band and an electrolyte membrane response frequency band, the anode electrode response frequency band being a frequency band which shows responsiveness to a state quantity of the anode electrode of the fuel cell, the electrolyte membrane response frequency band being a frequency band higher than the anode electrode response frequency band and which shows responsiveness to a state quantity of an electrolyte membrane of the fuel cell; and

the impedance acquisition unit acquires at least either one of an anode electrode response impedance based on a frequency selected from the anode electrode response frequency band and an electrolyte membrane response impedance based on a frequency selected from the electrolyte membrane response frequency band as the high frequency impedance.

**17**. The state detection device for the fuel cell according to claim **16**, wherein:

the impedance acquisition unit acquires both the anode electrode response impedance and the electrolyte membrane response impedance as the high frequency impedances; and

the internal state quantity estimation unit estimates the state quantity of the electrolyte membrane on the basis of the electrolyte membrane response impedance and estimates the state quantity of the anode electrode on the basis of the estimated state quantity of the electrolyte membrane and the anode electrode response impedance.

**18**. The state detection device for the fuel cell according to claim **16**, wherein:

the impedance acquisition unit acquires only the anode electrode response impedance as the high frequency impedance; and

the internal state quantity estimation unit estimates the state quantity of the anode electrode on the basis of the anode electrode response impedance.

**19**. The state detection device for the fuel cell according to claim **17**, wherein:

the state quantity of the anode electrode include a reaction resistance value and an electrical double layer capacitance value of the anode electrode;

the state quantity of the cathode electrode include a reaction resistance value and an electrical double layer capacitance value of the cathode electrode; and

the internal state quantity estimation unit:

estimates the reaction resistance value of the anode electrode and the electrical double layer capacitance value of the anode electrode on the basis of the anode electrode response impedance; and

estimates at least either one of the reaction resistance value and the electrical double layer capacitance value of the cathode electrode on the basis of the estimated state quantity of the electrolyte membrane, reaction resistance value of the anode electrode, electrical double layer capacitance value of the anode electrode and the low frequency impedance.

**20**. The state detection device for the fuel cell according to claim **14**, wherein:

the impedance acquisition unit acquires a value of a gradient in an I-V characteristic curve of the fuel cell as the low frequency impedance.

**21**. The state detection device for the fuel cell according to claim **20**, wherein:

the impedance acquisition unit acquires the value of the gradient as the low frequency impedance in steady time during which a variation of the value of the gradient in the I-V characteristic curve of the fuel cell is not larger than a predetermined value.

**22**. The state detection device for the fuel cell according to claim **20**, wherein:

the gradient in the I-V characteristic curve is calculated on the basis of two sets of measurement values of a current and a voltage.

**23**. The state detection device for the fuel cell according to claim **20**, wherein:

the gradient in the I-V characteristic curve is calculated on the basis of one set of measurement values of a current and a voltage and one set of current and voltage values set beforehand.

**24**. The state detection device for the fuel cell according to claim **14**, wherein:

the fuel cell is configured as a laminated battery; and

the state detection device comprises:

an alternating-current power supply unit connected to the laminated battery and configured to output an alternating current to the laminated battery;

an alternating current adjustment unit configured to adjust the alternating current on the basis of a positive electrode side alternating-current potential difference and a negative electrode side alternating-current potential difference, the positive electrode side alternating-current potential difference being a potential difference obtained by subtracting a potential of an intermediate part of the laminated battery from a potential on a positive electrode side of the laminated battery, the negative electrode side alternating-current potential difference being a potential difference obtained by subtracting the potential of the intermediate part of the laminated battery from a potential on a negative electrode side of the laminated battery; and

an impedance calculation unit configured to calculate an impedance measurement value of the fuel cell on the basis of the adjusted alternating current and the positive electrode side alternating-current potential difference and the negative electrode side alternating-current potential difference.

**25**. The state detection method for the fuel cell according to claim **13**, wherein the internal state quantity estimation:

estimates a certain internal state quantity on the basis of the high frequency impedance and estimates another internal state quantity on the basis of the estimated internal state quantity and the low frequency impedance; or

estimates a certain internal state quantity on the basis of the low frequency impedance and estimates another internal state quantity on the basis of the estimated internal state quantity and the high frequency impedance.

**26**. The state detection method for the fuel cell according to claim **13**, wherein the high frequency band includes an anode electrode response frequency band and an electrolyte membrane response frequency band, the anode electrode response frequency band being a frequency band which shows responsiveness to a state quantity of the anode electrode of the fuel cell, the electrolyte membrane response frequency band being a frequency band higher than the anode electrode response frequency band and which shows responsiveness to a state quantity of an electrolyte membrane of the fuel cell; and

at least either one of an anode electrode response impedance based on a frequency selected from the anode electrode response frequency band and an electrolyte membrane response impedance based on a frequency selected from the electrolyte membrane response frequency band as the high frequency impedance is acquired.

**27**. The state detection method for the fuel cell according to claim **26**, wherein:

both the anode electrode response impedance and the electrolyte membrane response impedance are acquired as the high frequency impedances; and

the state quantity of the electrolyte membrane is estimated on the basis of the electrolyte membrane response impedance and the state quantity of the anode electrode is estimated on the basis of the estimated state quantity of the electrolyte membrane and the anode electrode response impedance.

**28**. The state detection method for the fuel cell according to claim **26**, wherein:

only the anode electrode response impedance is acquired as the high frequency impedance; and

the state quantity of the anode electrode is estimated on the basis of the anode electrode response impedance.

**29**. The state detection method for the fuel cell according to claim **27**, wherein:

the state quantity of the anode electrode include a reaction resistance value and an electrical double layer capacitance value of the anode electrode;

the state quantity of the cathode electrode include a reaction resistance value and an electrical double layer capacitance value of the cathode electrode; and

the internal state quantity estimation:

estimates the reaction resistance value of the anode electrode and the electrical double layer capacitance value of the anode electrode on the basis of the anode electrode response impedance; and

estimates at least either one of the reaction resistance value and the electrical double layer capacitance value of the cathode electrode on the basis of the estimated state quantity of the electrolyte membrane, reaction resistance value of the anode electrode, electrical double layer capacitance value of the anode electrode and the low frequency impedance.

**30**. The state detection method for the fuel cell according to claim **13**, wherein:

a value of a gradient in an I-V characteristic curve of the fuel cell is acquired as the low frequency impedance.

**31**. The state detection method for the fuel cell according to claim **30**, wherein:

the value of the gradient as the low frequency impedance in steady time during which a variation of the value of the gradient in the I-V characteristic curve of the fuel cell is not larger than a predetermined value is acquired.

**32**. The state detection method for the fuel cell according to claim **30**, wherein:

the gradient in the I-V characteristic curve is calculated on the basis of two sets of measurement values of a current and a voltage.

**33**. The state detection method for the fuel cell according to claim **30**, wherein:

the gradient in the I-V characteristic curve is calculated on the basis of one set of measurement values of a current and a voltage and one set of current and voltage values set beforehand.

**34**. The state detection method for the fuel cell according to claim **13**, wherein:

the fuel cell is configured as a laminated battery; and

the method uses a state detection device which comprises:

an alternating-current power supply unit connected to the laminated battery and configured to output an alternating current to the laminated battery;

an alternating current adjustment unit configured to adjust the alternating current on the basis of a positive electrode side alternating-current potential difference and a negative electrode side alternating-current potential difference, the positive electrode side alternating-current potential difference being a potential difference obtained by subtracting a potential of an intermediate

part of the laminated battery from a potential on a positive electrode side of the laminated battery, the negative electrode side alternating-current potential difference being a potential difference obtained by subtracting the potential of the intermediate part of the laminated battery from a potential on a negative electrode side of the laminated battery; and

an impedance calculation unit configured to calculate an impedance measurement value of the fuel cell on the basis of the adjusted alternating current and the positive electrode side alternating-current potential difference and the negative electrode side alternating-current potential difference.

* * * * *